J. Fluid Mech. (1997), *vol.* 338, *pp.* 249–276

Printed in the United Kingdom © 1997 Cambridge University Press

Eulerian and Lagrangian velocity correlations in two-dimensional random geostrophic flows

By H. L. PÉCSELI[1] AND J. TRULSEN[2]

[1]Institute of Physics, University of Oslo, Box 1048 Blindern, N-0316 Oslo, Norway

[2]Institute of Theoretical Astrophysics, University of Oslo, Box 1029 Blindern, N-0315 Oslo, Norway

(Received 2 October 1995 and in revised form 2 December 1996)

Random flows in rotating fluid layers are studied in two spatial dimensions. The Eulerian and Lagrangian correlation functions for such flows are analysed by approximating the actual two-dimensional flow by an autonomous system consisting of many overlapping and mutually convecting vortices. Analytical expressions for the full space–time-varying Eulerian velocity correlation are derived solely in terms of flow parameters. An extension of the arguments giving these results also allows the derivation of analytical expressions for the Lagrangian velocity correlation function. The analytical results are supported by a numerical simulation.

1. Introduction

The basic properties of low-frequency fluctuations in a rotating flow layer can be described by the nonlinear set of equations

$$\frac{\partial \boldsymbol{v}}{\partial t} + \boldsymbol{v}\cdot\nabla\boldsymbol{v} = -g\nabla h - 2\boldsymbol{\Omega}\times\boldsymbol{v}, \tag{1.1}$$

expressing the acceleration of a fluid element in terms of the gradient of the hydrostatic pressure $p = \rho g h$ and the Coriolis force, ignoring a viscosity term and friction with the supporting bottom surface. In addition there is the equation of continuity, which here takes the form

$$\frac{\partial h}{\partial t} + \nabla\cdot(h\boldsymbol{v}) = 0, \tag{1.2}$$

where $\boldsymbol{v} = \boldsymbol{v}(\boldsymbol{r}, t)$ is the horizontal velocity being a function of time t, the position vector is $\boldsymbol{r} = \{x, y\}$, h is the local depth of the fluid layer, g is the acceleration due to gravity and $\boldsymbol{\Omega}$ is the angular velocity of the rotation. The analysis is carried out in two spatial dimensions with the restriction that all relevant horizontal scales are much larger than h. Rewriting (1.1) as

$$\boldsymbol{v} = -g\frac{\nabla h\times\boldsymbol{\Omega}}{2\Omega^2} + \frac{1}{2\Omega^2}\left(\frac{\partial}{\partial t} + \boldsymbol{v}\cdot\nabla\right)(\boldsymbol{\Omega}\times\boldsymbol{v}), \tag{1.3}$$

the first approximation for $\boldsymbol{v}$ has the form

$$\boldsymbol{v} = -g\frac{\nabla h\times\boldsymbol{\Omega}}{2\Omega^2}, \tag{1.4}$$

valid in the limit of large Ω. The vertical fluid displacement h here takes the role of a stream function for the flow. Within this approximation a fluid element is inertialess and assumes the velocity $\boldsymbol{v}$ instantaneously when released in the flow.

Taking the first iteration, by inserting (1.4) in the right-hand side of (1.3) the standard result is obtained

$$\frac{\partial}{\partial t}\left(\nabla^2\eta - \frac{1}{\lambda_R^2}\eta\right) - 2\Omega\lambda_R^2(\nabla\eta \times \hat{\boldsymbol{e}})\cdot\nabla\nabla^2\eta = 0, \tag{1.5}$$

with $\eta \equiv \tilde{h}/h_0$ where $h = h_0 + \tilde{h}$ was introduced with h_0 being the unperturbed fluid depth. The unit vector $\hat{\boldsymbol{e}}$ is in the $\boldsymbol{\Omega}$-direction. Only terms up to second order were retained to be consistent with the iteration. The equation is characterized by the spatial scale (the Rossby radius) $\lambda_R = (gh_0)^{1/2}/(2\Omega)$. The model equation is inherently nonlinear; if the equations are linearized, the trivial statement $\partial\eta/\partial t = 0$ results. The equation is a special case of the Charney equation (Charney 1948), which has been widely used for analysing the motion of, for instance, flows on a rotating planet. The applicability of the equation to other problems was discussed by e.g. Hasegawa, MacLennan & Kodama (1979) and Horton & Hasegawa (1994).

1.1. *Discussion of the model flow*

Since $(\nabla\eta \times \hat{\boldsymbol{e}})\cdot\nabla\eta = 0$, equation (1.5) is readily rewritten as

$$\frac{\partial}{\partial t}\zeta + \boldsymbol{v}\cdot\nabla\zeta = 0, \tag{1.6}$$

with $\zeta = \nabla^2\eta - \eta/\lambda_R^2$. Equation (1.6) is the continuity equation for the scalar quantity $\zeta(\boldsymbol{r}, t)$ which in turns determines $\eta(\boldsymbol{r}, t)$ and the self-consistent incompressible velocity field $\boldsymbol{v}(\boldsymbol{r}, t) = -2\Omega\lambda_R^2\nabla\eta(\boldsymbol{r}, t) \times \hat{\boldsymbol{e}}$. It follows that ζ is constant along the characteristics of (1.6). A vortex method for solving (1.5) is then readily found by approximating $\boldsymbol{v}(\boldsymbol{r}, t)$ by a velocity field generated by a collection of delta-functions whose support approximates that of ζ. Each of these delta-functions is convected by the net flow and contributes with a velocity field corresponding to a point vortex. The velocity $\boldsymbol{v}$ is calculated by a sum of the contributions from the vortices, where the contribution from an individual vortex with strength A is obtained from the solution of $\nabla^2\eta_\ell(\boldsymbol{r}) - \eta_\ell(\boldsymbol{r})/\lambda_R^2 = -A_\ell\delta(\boldsymbol{r} - \boldsymbol{r}_\ell)$. In two dimensions the solution is

$$\eta_\ell(\boldsymbol{r}) = (A_\ell/2\pi)K_0(|\boldsymbol{r} - \boldsymbol{r}_\ell|/\lambda_R), \tag{1.7}$$

where K_0 is the modified Bessel function of the second kind and zero order, as in the problem considered by Morikawa (1960).

The velocity deduced from the stream function (1.7) will have the form of a vortex. The flow field is expressed here in terms of a sum of velocity contributions from the individual vortices:

$$\boldsymbol{v}(\boldsymbol{r}, t) = \sum_{\ell=1}^{N} \boldsymbol{u}_\ell(\boldsymbol{r}). \tag{1.8}$$

An autonomous model is obtained by requiring that individual structures are convected by the flow generated by all the others,

$$\frac{\mathrm{d}\boldsymbol{r}_\ell(t)}{\mathrm{d}t} = \sum_{k\neq\ell}^{N} \boldsymbol{u}_k(\boldsymbol{r}_\ell). \tag{1.9}$$

Equations (1.8) and (1.9) are conveniently rewritten as

$$\boldsymbol{v}(\boldsymbol{r},t) \;=\; -2\Omega\lambda_R^2\nabla\Phi\times\hat{\boldsymbol{e}} \;=\; -2\Omega\lambda_R^2\sum_{k=1}^{N}\nabla\eta_k(\boldsymbol{r})\times\hat{\boldsymbol{e}}, \tag{1.10}$$

and

$$\frac{\mathrm{d}\boldsymbol{r}_\ell(t)}{\mathrm{d}t} \;=\; -2\Omega\lambda_R^2\sum_{k\neq l}^{N}\nabla\eta_k(\boldsymbol{r}_\ell)\times\hat{\boldsymbol{e}}. \tag{1.11}$$

The introduction of the stream function, $\Phi = \sum_{k=1}^{N}\eta_k(\boldsymbol{r})$, ensures that the flow is incompressible, $\nabla\cdot\boldsymbol{v}(\boldsymbol{r},t) = 0$. Onsager's (1949) line-vortex model is a special case of (1.10)–(1.11) with the choice $\eta_k(\boldsymbol{r}) = A_k\ln(|\boldsymbol{r}|)$. Formally, this case can be obtained by retaining only the $\ln(r)$ term in an expansion of $K_0(r)$.

It is well known that the dynamic system of structures described by (1.10)–(1.11) can be put in a Hamiltonian form. Introducing $\eta_k = A_kF(|\boldsymbol{r}|)$, where $F(r)$ can be taken as an arbitrary function and A_k is a constant, the result is

$$H \;=\; \sum_{\ell>k} A_\ell A_k F(|\boldsymbol{r}_\ell - \boldsymbol{r}_k|)\;. \tag{1.12}$$

The conservation of the Hamiltonian (1.12) is not restricted to particular choices of F such as $K_0(r)$ or $\ln(r)$. We use here the general form F to emphasize that the Hamiltonian property is retained, even when the singularity of the K_0-function is smoothed out for practical applications. The Hamiltonian (1.12) accounts for an effective potential energy of the interacting structures. This is made evident by considering the particular line vortex model. The system does not possess kinetic energy in the usual sense. The Hamiltonian (1.12) applies in the absence of boundaries. The presence of for instance periodic boundary conditions requires the introduction of a modified expression for F.

From the construction it is clear that individual structures, as specified by η_k in (1.10) and (1.11) or by F in (1.12), are not distorted by the flow. However, any macroscopic arrangement of many individual structures will be distorted and sheared by the flow. The velocity field, (1.10), will therefore have properties in common with flows evolving according to the two-dimensional Euler equations. Any flow described by (1.10) with a smooth initial condition (implying smooth basic vortices $F(r)$ in (1.12)) will remain smooth for all later times, i.e. no discontinuities will develop. These properties are consistent with those characterizing flows described by the Euler equation in two dimensions. A general review of vortex methods is given by for instance Leonard (1980) or Sarpkaya (1989), where the present model represents a special case. Our modelling of the flow by a superposition of vortices is of course not unique, for instance for a driven dissipative system a kinetic simulation as used by e.g. Fung *et al.* (1992) may be advantageous.

The paper is organized as follows. In §2 we discuss the applications of the model for describing turbulent diffusion. In §3 a simplified derivation is presented for results first obtained by Wandel & Kofoed-Hansen (1962) for the case of two-dimensional flows. Particular emphasis is given to the time variation of the Eulerian and Lagrangian velocity auto-correlation functions. In §4 the limitations of this analysis are pointed out and a remedy, based on conditional averaging of the fluctuating velocity, is suggested. In §5 the numerical scheme for the simulations is discussed and results are compared with the analytical expressions. Finally §6 contains our conclusions.

2. Turbulent diffusion

The model discussed in the introduction is applied to the study of turbulent transport, in particular to the dispersion of a test particle with respect to its origin of release. Even for idealized conditions, where homogeneous isotropic turbulence is considered, this is a rather complicated problem. Readily measurable quantities such as correlation functions are Eulerian, i.e. they are obtained in fixed positions or with probes moving along prescribed trajectories. However, the relevant statistical information needed for analysing particle dispersion is Lagrangian, i.e. obtained along particle orbits. Consequently, the analysis of turbulent transport can be considered as deriving the desired Lagrangian statistical quantities on the basis of measured Eulerian characteristics of the random fluctuations.

The simplest relevant quantity describing the motion of a particle is its mean-square displacement, $\langle r^2 \rangle$, with respect to its initial position. For short times after release we have $\boldsymbol{r} \approx \boldsymbol{v}\, t$, i.e.

$$\langle r^2 \rangle \approx \langle v_L^2 \rangle\, t^2\,, \tag{2.1}$$

where $\langle v_L^2 \rangle$ is the mean-square Lagrangian velocity, to be determined by sampling along particle orbits. Equation (2.1) shows that the transport is convection dominated for small time scales. For incompressible flows (Tennekes & Lumley 1972), the mean-square velocity obtained by Eulerian sampling, $\langle v_E^2 \rangle$, is identical to the mean-square velocity, $\langle v_L^2 \rangle$, obtained from Lagrangian measurements. In this case the evaluation of (2.1) becomes simple. The subscripts on $\langle v^2 \rangle$ will be omitted from here on. For arbitrary times, $\langle r^2 \rangle$ is expressed in terms of the Lagrangian velocity correlation function $R_L(\tau) = \langle \boldsymbol{v}(\boldsymbol{r}(t)) \cdot \boldsymbol{v}(\boldsymbol{r}(t+\tau)) \rangle / \langle v^2 \rangle$ as

$$\langle r^2 \rangle = 2\langle v^2 \rangle t \int_0^t (1 - \tau/t) R_L(\tau) \mathrm{d}\tau\,, \tag{2.2}$$

which contains (2.1) in the limit of small t where $R_L(\tau) \simeq 1$. For large times, $t \gg \tau_L$, (2.2) gives a diffusion-like dispersion

$$\langle r^2 \rangle \approx 2\langle v^2 \rangle \tau_L\, t\,, \tag{2.3}$$

where $\tau_L \equiv \int_0^\infty R_L(\tau)\mathrm{d}\tau$ is the Lagrangian integral time scale. An early attempt to make predictions directly for the correlation function was made by Hay & Pasquill (1960). Later, Wandel & Kofoed-Hansen (1962) provided a theoretical basis for their hypothesis. Rather than considering an actual turbulent flow as described by the three-dimensional Navier–Stokes equation, Wandel & Kofoed-Hansen approached the problem using an autonomous system, which for certain parameters have turbulence-like features. Their results were recognized in the literature (see e.g. Panofsky & Dutton 1984; McComb 1990).

In the present study we perform a numerical solution of a model which approximates the two-dimensional Euler equations for initial conditions which generate isotropic homogeneous random flows. Numerical results are compared with analytical expressions for the Eulerian as well as the Lagrangian correlation functions. A particularly interesting feature of the analysis of Wandel & Kofoed-Hansen (1962) and its extensions is that it also suggests an expression for the temporal variation of the Eulerian correlation for a given wavenumber spectrum, $E(k)$, and the variance, $\langle v^2 \rangle$, of the velocity fluctuations. The analysis of Wandel & Kofoed-Hansen (1962) will be considered and some of its shortcomings pointed out. The convection of passive test particles by a collection of unshielded point vortices was investigated for instance by Babiano *et al.* (1994) although with an emphasis different from the one in the present work.

3. Analytical results in two spatial dimensions

The present analysis is based on the assumption that the vortices are placed randomly in the plane. The probability of finding a vortex in a small rectangle $\mathrm{d}x\mathrm{d}y$ is assumed to be $\mu \mathrm{d}x\mathrm{d}y$, where μ is the density of vortices, independent of the positions of all the other vortices. This random distribution can be imposed initially. It is then assumed that this random spatial distribution also prevails during the subsequent temporal evolution. With this assumption the probability densities and correlation functions of the fluctuating flow velocity are readily obtained by standard methods (Rice 1944, 1945). The approximation can be justified in the limit of many overlapping vortices, i.e. the limit where the flow is characterized by many degrees of freedom. Here it can be argued that a small subset of the vortices can be removed from the flow without significantly changing its statistical properties, see also the discussion in Appendix A. In particular, if vortices which at a certain instance have velocities and positions in a small volume element around $\boldsymbol{v}_0$ and $\boldsymbol{r}_0$, are decoupled from the interaction, we might expect that the overall flow statistics remain unchanged. In this sense a weak statistical coupling between vortices can be argued for small values of $|H|$. The assumption clearly breaks down for a low vortex density. The assumption of 'weak independence' outlined here has implications for the prediction of measurable quantities and the conjecture can therefore be tested *a posteriori*. See also the discussion in the Conclusions.

3.1. *Probability densities*

For the following analysis it is natural to assume that both polarities of a vortex (high- and low-pressure) are equally probable. The two polarities will have opposite angular rotations. With the assumption that the positions of the vortices are independent, the probability density for the stream function is readily obtained by standard methods (Rice 1944):

$$P(\Phi) = \frac{1}{2\pi} \int_{-\infty}^{\infty} \exp\left(-\mathrm{i}\Phi\gamma + \mu \int_{-\infty}^{\infty} \{\cos[\gamma\eta(\boldsymbol{r})] - 1\} \mathrm{d}\boldsymbol{r} \right) \mathrm{d}\gamma, \tag{3.1}$$

where the basic structure η was introduced in (1.7). Here and in the following we use the abbreviation $\int_{-\infty}^{\infty} \mathrm{d}\boldsymbol{r}$ for $\int_{-\infty}^{\infty}\int_{-\infty}^{\infty} \mathrm{d}x\mathrm{d}y$. The density of structures $\mu = \langle N \rangle / L^2$ is introduced in terms of the average number, $\langle N \rangle$, of structures in the realizations. Similar expressions for the probability densities for the two velocity components, $P(v_x)$ and $P(v_y)$, are readily obtained. It can be demonstrated analytically (Rice 1944) that $P(v_y)$ approaches a Gaussian distribution when $\mu \to \infty$ as expected from the central limit theorem. Two-point distribution functions and also higher-order distributions can be obtained similarly. These approach multidimensional Gaussian distributions in the limit $\mu \to \infty$.

3.2. *Spatial correlations*

The elements of the two-point velocity correlation tensor

$$R_{j\ell}(\boldsymbol{\xi}) \equiv \langle v_j(\boldsymbol{r}) v_\ell(\boldsymbol{r} - \boldsymbol{\xi}) \rangle = g(\xi)\delta_{jl} + [f(\xi) - g(\xi)]\, \xi_j \xi_\ell / \xi^2$$

associated with the model (1.10)–(1.11) can be expressed in terms of the corresponding correlation function for the stream function $R_\Phi(\boldsymbol{\xi})$. The longitudinal and lateral correlation functions are given by $f = -(1/\xi)\mathrm{d}_\xi R_\Phi(\xi)$ and $g = -\mathrm{d}_\xi^2 R_\Phi(\xi)$, respectively. The implied relation $g = \partial_\xi(\xi f)$ will also remain valid when the full space–time variation of $f(\xi, \tau)$ and $g(\xi, \tau)$ is considered. Note that isotropic and homogeneous two-dimensional turbulence does not possess a lateral integral scale

length, $\int_0^\infty g(\xi)\mathrm{d}\xi = 0$. This merely states that back flow is necessary somewhere in the plane; $g(\xi)$ must become negative for some values of ξ in order to keep the net flux zero. A longitudinal integral scale length can, however, be obtained as $\ell_E \equiv \int_0^\infty f(\xi)\mathrm{d}\xi$.

The correlation function for the stream function can in turn be calculated directly without use of the two-point distribution function. With the assumption that both polarities of a vortex are equally probable, the correlation function of the stream function becomes simply (Rice 1944)

$$R_\Phi(\boldsymbol{\xi}) = \mu \int_{-\infty}^{\infty} \eta(\boldsymbol{r})\eta(\boldsymbol{r}-\boldsymbol{\xi})\mathrm{d}\boldsymbol{r}, \tag{3.2}$$

where μ now represents the density of vortices irrespective of polarity. The isotropy of η implies that $R_\Phi(\boldsymbol{\xi}) = R_\Phi(\xi)$. The correlation $R_\Phi(\xi)$ is unaffected by the transition to the Gaussian limit for $\mu \to \infty$, provided the amplitudes of the individual structures go to zero simultaneously so that the mean-square fluctuation level remains constant.

The wavenumber spectrum of the random spatial stream function variation is obtained by Fourier transforming the corresponding correlation function. Denoting this spectrum $E_\Phi(\boldsymbol{k})$, the elements of the velocity power spectral tensor are readily expressed as

$$E_{j\ell}(\boldsymbol{k}) = k^2 E_\Phi(\boldsymbol{k}) \left[\delta_{j\ell} - \frac{k_j k_\ell}{k^2}\right]. \tag{3.3}$$

From here on we assume that a constant $4\Omega^2\lambda_R^4$ is included in E_Φ. With the definition (3.3), the energy density is obtained from $\int_{-\infty}^{\infty} E_{jj}(\boldsymbol{k})\mathrm{d}\boldsymbol{k}$ using the summation convention. For the present problem where the basic vortex structure is described by $\eta(\boldsymbol{r}, t) = (A/2\pi)K_0(|\boldsymbol{r}|/\lambda_R)$, we find after some elementary algebra the power spectrum

$$E_\Phi(\boldsymbol{k}) = \frac{C}{(1+(k\lambda_R)^2)^2}, \tag{3.4}$$

where C is a constant determined by the actual flow parameters including the energy density. The corresponding velocity power spectrum becomes

$$E(\boldsymbol{k}) \equiv E_{jj}(\boldsymbol{k}) = k^2 E_\Phi(\boldsymbol{k}) = \frac{Ck^2}{(1+(k\lambda_R)^2)^2}. \tag{3.5}$$

The divergence of the integral over all k is associated with the singularity at the origin of the basic vortex determined by the derivative of the K_0-function, where $\mathrm{d}K_0(r)/\mathrm{d}r = -K_1(r)$. For realistic models this singularity will be remedied by rounding-off the K_0-function at its origin. In figure 1 we give the analytical wavenumber spectrum obtained for the model used in the present study. The results for two different cut-offs are illustrated. As the cut-off radius decreases, the velocity spectrum develops a $1/k^2$-subrange.

It is interesting that using thermodynamic arguments for a truncated spectral representation with discrete wavenumbers, Hasegawa *et al.* (1978) obtained an equilibrium spectrum for the stream function of the form

$$E_\Phi(\boldsymbol{k}) = \frac{C}{(1+(k\lambda_R)^2)(\alpha+\beta(k\lambda_R)^2)}, \tag{3.6}$$

with α^{-1} and β^{-1} being two temperatures and where one can attain negative values. There is here no divergence in the integrated velocity spectrum because of the implied truncation in wavenumbers. The result (3.4) does not imply any such truncation,

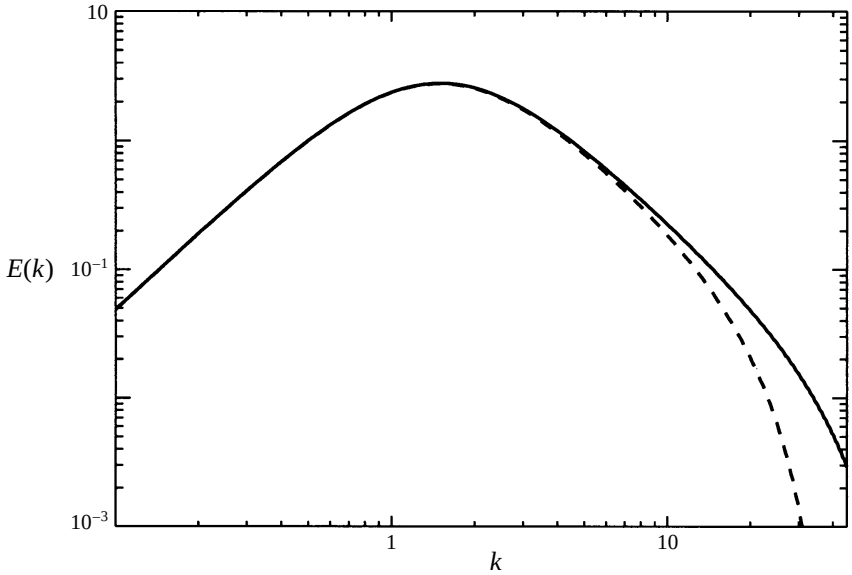

FIGURE 1. Analytically obtained power spectrum $E(k)$ as function of wavenumber for the fluctuations in velocity. The solid line shows the case used in this work where the singularity of the K_0-function is removed by a parabolic fit within a circle with radius 0.05 around the origin of the vortices, for the dashed line the radius is 0.1.

but it is interesting to note that it coincides with (3.6) for the case where $\alpha = \beta$. The derivation of (3.6) is based on the conservation of energy and an equivalent of enstrophy for a system described by the basic equation (1.5). In order to recover a spectrum like (3.6) with $\alpha \neq \beta$, the analysis of a discrete vortex model must be based on a probability density for the spatial distribution which has a preference for the sign of the nearest-neighbour vortices. This analysis has not been carried out.

The standard model for the unshielded line vortex model can be obtained in the limit where $\lambda_R \to \infty$ giving $E_\Phi(\boldsymbol{k}) = C/k^4$ or $E(\boldsymbol{k}) = C/k^2$. The integral over the spectrum for the unshielded vortices receives a diverging contribution both for large and for small wavenumbers. The spectra for the two models are equivalent for large wavenumbers, differences appearing for $k \leqslant 1/\lambda_R$.

3.3. *The Eulerian correlation function*

Consider first the normalized spatial correlation function expressed as the Fourier transform of the reduced velocity power spectrum

$$\begin{aligned} R(\boldsymbol{r}) \equiv R_{jj}(\boldsymbol{r}) &= f(r) + g(r) \\ &= \frac{1}{2\pi\sigma^2} \int_{-\infty}^{\infty} E(\boldsymbol{k}) \mathrm{e}^{\mathrm{i}\boldsymbol{k}\cdot\boldsymbol{r}} \, \mathrm{d}\boldsymbol{k} \,. \end{aligned} \tag{3.7}$$

From here on we assume the normalization $R(0) = 1$, and therefore also $f(0) = g(0) = 1/2$. Consider now a frozen velocity field, with all vortices at fixed positions, being swept with constant velocity $\boldsymbol{u}$ past a stationary observer. A correlation function $R_u(t)$ is obtained by correlating the velocities at the reference position at two different times separated by t,

$$R_{\boldsymbol{u}}(t) = \frac{1}{2\pi\sigma^2} \int_{-\infty}^{\infty} E(\boldsymbol{k}) \mathrm{e}^{\mathrm{i}\boldsymbol{k}\cdot\boldsymbol{u}t} \, \mathrm{d}\boldsymbol{k} \,. \tag{3.8}$$

This case corresponds to having $\boldsymbol{r}_\ell = \boldsymbol{r}_{0\ell} + \boldsymbol{u}t$ in (1.8) with $\boldsymbol{r}_{0\ell}$ being uniformly distributed in space. In the actual flow different groups of vortices can be distinguished by having different velocities, but each group has the same wavenumber spectrum $E(\boldsymbol{k})$ and associated spatial correlation function given by (3.7). The one-point two-time velocity correlation function is now approximated by sum of the respective individual correlations given by (3.8), summed over all velocities u. This summation is the basic assumption of our analysis. It is exact if the various groups can be considered independent. Physically it can be justified if one group of vortices, all with velocities within a narrow range, can be removed from the flow without significantly affecting its overall statistical properties. Clearly, this can never be justified for small vortex densities, and therefore only the limit μ large will be considered in the following.

In the actual flow the vortex velocities $\boldsymbol{u}$ are statistically distributed. Their probability density is a measurable quantity and has an explicit analytical expression similar to (3.1) within the present approximations. Particularly, in the limit of $\mu \to \infty$, this probability density can safely be assumed to be a Gaussian with zero mean and variance $\sigma^2 = (1/2\pi)\int_{-\infty}^{\infty} E(\boldsymbol{k})\,\mathrm{d}\boldsymbol{k}$. After averaging over all values of $\boldsymbol{u}$ the expectation value for $R(t)$ consequently becomes

$$\begin{aligned} R(t) &= \frac{1}{2\pi\sigma^2}\int_{-\infty}^{\infty} E(\boldsymbol{k})\langle \mathrm{e}^{\mathrm{i}\boldsymbol{k}\cdot\boldsymbol{u}t}\rangle\,\mathrm{d}\boldsymbol{k} \\ &= \frac{1}{2\pi\sigma^2}\int_{-\infty}^{\infty} E(\boldsymbol{k})\int_{-\infty}^{\infty} \mathrm{e}^{\mathrm{i}\boldsymbol{k}\cdot\boldsymbol{u}t} P(\boldsymbol{u})\,\mathrm{d}\boldsymbol{u}\,\mathrm{d}\boldsymbol{k} \\ &= \frac{1}{\sigma^2}\int_0^{\infty} E(k)\mathrm{e}^{-(\sigma k t)^2/4} k\,\mathrm{d}k\,, \end{aligned} \tag{3.9}$$

with $P(\boldsymbol{u}) = (\pi\sigma^2)^{-1}\exp(-u^2/\sigma^2)$. More generally we can determine the entire space–time-varying correlation function, obtainable by correlating velocity fluctuations at two fixed spatial positions with separation r at two times with relative delay t. With the assumption of random translations with constant but random velocities, as in (3.9), the result is

$$R_E(r,t) = \frac{1}{\sigma^2}\int_0^{\infty} E(k)J_0(kr)\mathrm{e}^{-(\sigma k t)^2/4} k\mathrm{d}k\,, \tag{3.10}$$

where the subscript E emphasizes the Eulerian sampling of the fluctuations. The result (3.10) corresponds to the one obtained by Wandel & Kofoed-Hansen (1962), but the underlying arguments were also proposed earlier by Kraichnan (1959). The interesting aspect of this result, shown in figure 2(*a*), is that it allows a prediction of the full space–time-varying Eulerian correlation function on the basis of the energy spectrum, $E(k)$, alone. For $t = 0$ expression (3.10) is just a different presentation of (3.8). Note the time scaling σt implied in (3.10), i.e. an increase in the standard deviation σ by an increase in energy density of the fluctuations can be accounted for simply by rescaling the temporal variable.

3.4. *The Lagrangian velocity correlation function*

The arguments can now be applied in the same way for the Lagrangian correlation function. First we consider the limiting case of a frozen flow, where the velocity field is formally taken to be a function of position only. This extreme case is similar to the one argued to derive (3.9), since the expression does not distinguish between a moving flow and a fixed observer or a fixed (i.e. frozen) flow and a moving particle. The result in (3.9) is thus also applicable, with the present arguments, for the Lagrangian correlation $R_L(t)$ for frozen flows.

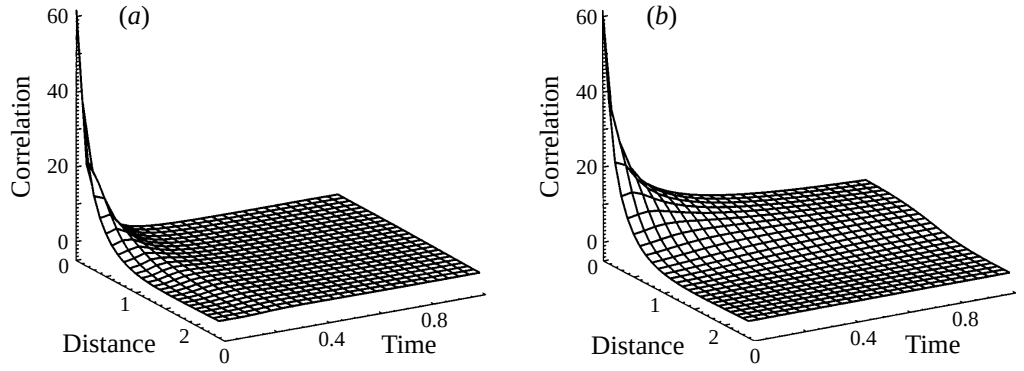

FIGURE 2. Analytical result for the Eulerian correlation functions for the parameters $\lambda_R = 2/3$ and $\mu = 12$, for vortices of strength $\pm 1/\sqrt{3}$: (*a*) the result based on an approximation used by Wandel & Kofoed-Hansen see (3.10), (*b*) result obtained by numerical solution of (4.5)–(4.6). The correlation functions are shown in their unnormalized form to also bring out the analytical value of $\langle v^2 \rangle$ given by the functional values at the origin. The Eulerian length scale is obtained numerically as $\ell_E \approx 0.81$.

We now let the vortices surrounding the test particle be moving also, i.e. the local velocity at the test particle position $\boldsymbol{r}(t)$ becomes an explicit function of time, $\boldsymbol{v}(\boldsymbol{r}(t), t)$. The velocities of test particles with respect to vortices are no longer the same as their rest-frame velocities, and it is the distribution of relative velocities which is needed when estimating the temporal variation in velocity experienced when the test particle passes the individual vortices constituting the flow.

It can safely be assumed that the statistical distribution of the velocities of the vortices constituting the flow surrounding the test particle is a Gaussian just like that of the test particles themselves and with the same standard deviation, σ. Following Wandel & Kofoed-Hansen (1962) we postulate that the distribution for the relative velocities, as an approximation, can also be taken to be a Gaussian, with standard deviation $\sigma\sqrt{2}$. This result would be exact for the case where the two velocities were independent. For distant vortices the assumption is easily justified, but for nearby vortices at relative distances $\leqslant \lambda_R$ the two velocities are correlated. The assumption thus amounts to ignoring this correlation, but only when estimating the characteristic function. The hypothesis can be tested by comparing the results it implies with numerical simulations of the problem. This comparison will be carried out in §5 of this paper.

With the present assumptions, the Lagrangian auto-correlation function becomes

$$R_L(t) = \frac{1}{\sigma^2} \int_0^\infty E(k) \mathrm{e}^{-(\sigma k t)^2/2} k \mathrm{d}k \,. \tag{3.11}$$

The results (3.9)–(3.11) are identical to those obtained on the basis of an analysis developed by Wandel & Kofoed-Hansen (1962) and Kofoed-Hansen & Wandel (1967) who presented their results in terms of component spectra. Their final expressions account for the dominating terms in a series expansion in a small parameter which they considered as being analogous to an effective Reynolds number, interpreted as the effective number of degrees of freedom for the flow. Note that the time scaling σt implied in (3.10) is retained in (3.11). The result (3.11) was obtained without explicit use of Corrsin's (1960) hypothesis, since for the present problem the spectrum $E(k)$ is obtained from the Fourier power transform of an individual structure, thus being

a deterministic quantity and therefore unaffected by the ensemble averaging. See also the discussion by Weinstock (1976). Elements of the foregoing analysis were proposed by Kraichnan (1959).

An interesting result of the foregoing analysis is that the micro time scales associated with the Eulerian and the Lagrangian correlation functions are related as $\tau_E = \sqrt{2}\tau_L$ to the present approximation, as obtained by comparing (3.10) and (3.11).

The results (3.10)–(3.11) are simple, but it was implicitly assumed that the characteristics of the flow change only little during the time it takes a fluid element to propagate a distance which characterizes the flow, typically an Eulerian integral scale length or in our case the width of a vortex. During this time interval a test particle is taken to follow a straight orbit, $\boldsymbol{r} \approx \boldsymbol{u}t$, corresponding to the limit (1.2). To be specific we can give an estimate for the error between the actual velocity a vortex will experience and the straight line orbit approximation used here. This error can be expressed as

$$\begin{aligned} e^2 &= \langle (\boldsymbol{u} - \boldsymbol{v}(\boldsymbol{r}(t), t))^2 \rangle \\ &= 2\langle v^2 \rangle (1 - R_L(t)). \end{aligned} \tag{3.12}$$

The averaging is performed over all realizations using that $\boldsymbol{u} = \boldsymbol{v}(\boldsymbol{r} = 0, t = 0)$ has the same statistical distribution as the flow velocity. For short times the error e is small and the approximation worth pursuing, i.e. the correlation functions may approximate the numerical results well for small time delays. In particular, the Taylor microscale may be well represented by the results. For large times, the error in the estimated velocity is $2\langle v^2 \rangle$. In this limit we expect a diffusion-like dispersion from (2.3), and the approximation $r \sim ut$ overestimates the displacement of the vortices with respect to their origin of release. Consequently $\exp(\mathrm{i}\boldsymbol{k} \cdot \boldsymbol{r})$ with $r \sim ut$ oscillates too rapidly in (3.9) and the integral therefore decreases too fast.

We can also directly estimate the displacement error e_r^2 in using $\boldsymbol{r} = \boldsymbol{u}t$ as an estimate for the actual displacement $\boldsymbol{r}$. We find after some simple algebra that

$$\begin{aligned} e_r^2 \equiv \langle (\boldsymbol{u}t - \boldsymbol{r}(t))^2 \rangle &= \langle u^2 \rangle t^2 + \langle r^2 \rangle - 2t\langle \boldsymbol{u} \cdot \boldsymbol{r}(t) \rangle \\ &= \langle v^2 \rangle \left(t^2 - 2 \int_0^t \tau R_L(\tau) \mathrm{d}\tau \right), \end{aligned} \tag{3.13}$$

where (2.2) was used, noting that $\langle u^2 \rangle = \langle v^2 \rangle$. For short times we approximate $R_L(\tau) \approx 1 - \frac{1}{2}\tau^2/T^2$ where T is the Lagrangian micro time scale. In this limit the t^2-terms cancel and (3.13) varies like $\frac{1}{4}\langle v^2 \rangle t^4/T^2$ and for times $t \ll T$ the approximation $r = ut$ is good. In the long time limit we have $e_r^2 \approx \langle v^2 \rangle t^2$ and the approximation is likely to be inadequate.

In order to improve the accuracy of our estimates for the velocity correlations at time separations comparable to or exceeding the Taylor microscale, we use an approximation based on conditionally averaged paths as proposed by Pécseli & Trulsen (1991*a*) see also Appendix A.

4. Conditionally averaged flows

To generalize and improve the results of the foregoing section, the ideal procedure would be to average all actual trajectories $\boldsymbol{r}(t)$ in the individual realizations when calculating the characteristic function. In principle this could be done by assuming that the velocity and its first N spatial derivatives are given at a certain position at a certain time t_0, with N being arbitrarily large. By a Taylor expansion, it is then

possible to estimate with arbitrary accuracy the (Eulerian) flow a test particle or a vortex will experience in the vicinity of its reference point, $\boldsymbol{r}_0$, at t_0 as well as at later times $t = \tau + t_0$. This estimate (or conditional average) is denoted $\check{\boldsymbol{v}}(\boldsymbol{r}_0 + \boldsymbol{r}, t_0 + \tau)$ and is a space–time-varying quantity with the actual (conditioned) flow field being $\boldsymbol{v}(\boldsymbol{r}_0 + \boldsymbol{r}, t)_c = \check{\boldsymbol{v}}(\boldsymbol{r}_0 + \boldsymbol{r}, t) + \boldsymbol{\vartheta}(\boldsymbol{r}_0 + \boldsymbol{r}, t)$, where $\boldsymbol{\vartheta}$ is a randomly varying correction, with $\boldsymbol{\vartheta}(\boldsymbol{r}_0, t_0) = 0$ in the conditionally selected subensemble. Evidently, the conditional average approximates the actual path better, the smaller the correction $\boldsymbol{\vartheta}$ is. The actual path of a passive test particle $\boldsymbol{r} = \boldsymbol{r}(t) = \int_{t_0}^{t} \boldsymbol{v}(\boldsymbol{r}_0 + \boldsymbol{r}(\tau), \tau)_c \, \mathrm{d}\tau$ relative to the initial position $\boldsymbol{r}_0$ in a given conditioned realization is approximated by the path which is obtained by integrating the velocity estimate $\check{\boldsymbol{v}}(\boldsymbol{r}_0 + \boldsymbol{r}, t)$ as suggested by Pécseli & Trulsen (1991*a*). Intuitively we expect this approximation to be improved as more terms are included in the Taylor expansion, i.e. higher-order derivatives are included in the imposed conditions. An approximation to the (unconditioned) characteristic function $\langle \exp[\mathrm{i}\boldsymbol{k} \cdot \boldsymbol{r}(t)] \rangle$ is subsequently obtained by averaging over all the imposed conditions. This averaging requires all relevant joint probability densities to be known. Within the present model these can in principle be obtained by the same calculations as used in deriving (3.1). To illustrate the procedure we use here the lowest-order approximation where a condition is imposed only on the magnitude of the velocity and its direction, leaving spatial and temporal derivatives unconditioned and the problems mentioned before do not arise. It is not *a priori* evident how many imposed conditions are necessary in order to have an adequate representation of the actual path in a given realization. It turns out, however, that the lowest-order approximation is sufficient to obtain a good agreement between theoretical correlation functions and those obtained from numerical simulations (Pécseli & Trulsen 1991*b*).

For the general case a series expansion for the kth component of $\check{\boldsymbol{v}}$ is introduced (Adrian 1979) as

$$\check{v}_k(\boldsymbol{r}_0 + \boldsymbol{r}, t_0 + \tau) = A_{k\ell}(\boldsymbol{r}, \tau) v_\ell(\boldsymbol{r}_0, t_0)_c + B_{k\ell m}(\boldsymbol{r}, \tau) v_\ell(\boldsymbol{r}_0, t_0)_c v_m(\boldsymbol{r}_0, t_0)_c + \cdots, \tag{4.1}$$

with $(\boldsymbol{r}_0, t_0)$ denoting the reference position and time and the velocity components entering the right-hand side refer to the imposed condition. There is no constant term in the series because of the assumed homogeneity and isotropy. Physically, $\check{\boldsymbol{v}}(\boldsymbol{r}_0 + \boldsymbol{r}, t_0 + \tau)$ is the average velocity at position $\boldsymbol{r}_0 + \boldsymbol{r}$, at time $t_0 + \tau$, given the condition that the velocity is $\boldsymbol{v}(\boldsymbol{r}_0, t_0)_c$ at the position $\boldsymbol{r}_0$ at time t_0. Retaining only the first term in the expansion (4.1), the coefficient tensor $A_{k\ell}(\boldsymbol{r}, \tau)$ is determined by minimizing the mean-square error

$$e_k^2 = \langle (\check{v}_k(\boldsymbol{r}_0 + \boldsymbol{r}, t_0 + \tau) - v_k(\boldsymbol{r}_0 + \boldsymbol{r}, t_0 + \tau))^2 \rangle, \tag{4.2}$$

for all k. The series expansion for $\check{v}_k$ given in (4.1) is inserted into (4.2) and the result minimized by requiring $\partial e_k^2 / \partial A_{k\ell} = 0$ for all k and ℓ, with details given by e.g. Adrian (1979). The result is expressed in terms of the Eulerian correlation function as

$$A_{k\ell}(\boldsymbol{r}, \tau) = \frac{1}{\sigma^2} \langle v_k(\boldsymbol{r}_0, t_0) v_\ell(\boldsymbol{r}_0 + \boldsymbol{r}, t_0 + \tau) \rangle \, . \tag{4.3}$$

For the case where the velocity fluctuations constitute a Gaussian random process, we obtain the exact result for the conditional average by retaining only the first term in the expansion, a limit considered also by Smith (1968). The present result is best expressed by introducing a stream function $\check{\Phi}(\boldsymbol{r}, t)$ so that the velocity estimate is $\check{\boldsymbol{v}}(\boldsymbol{r}, t) = \{\partial_y \check{\Phi}, -\partial_x \check{\Phi}\}$. The result is then

$$\check{\Phi} = 2\tilde{v} r f(r, \tau) \sin\theta \tag{4.4}$$

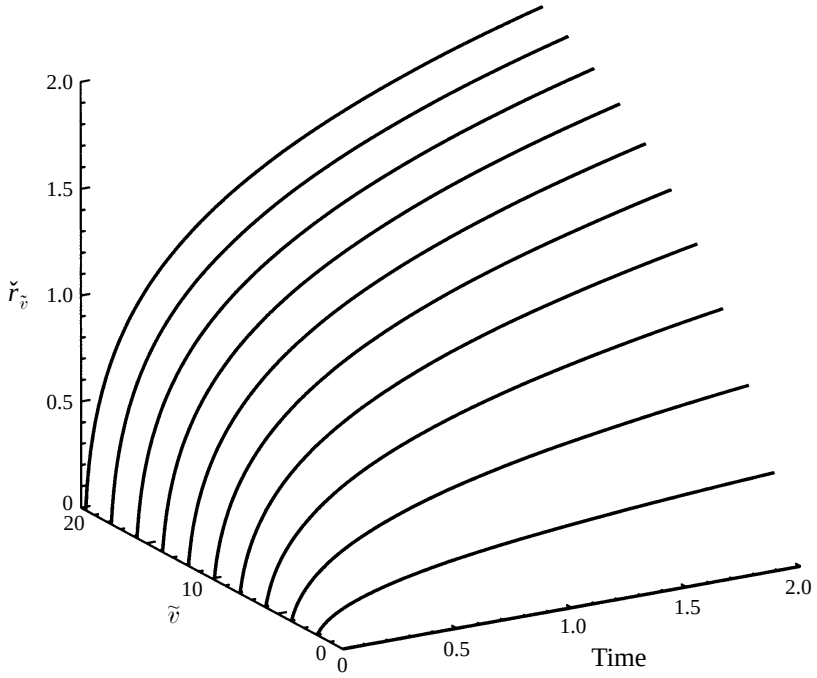

FIGURE 3. Time variation of $\check{r}_{\tilde{v}}(t)$ for different $\tilde{v}$. The standard deviation is $\langle v^2\rangle^{1/2} \approx 7.81$ for this particular case.

where $\tilde{v} = |\,\boldsymbol{v}(\boldsymbol{r}_0, t_0)_c\,|$ refers to the imposed condition, $f(r,\tau)$ is the normalized space–time-varying longitudinal correlation function, and θ is the angle with respect to the direction of the conditioned velocity $\boldsymbol{v}_c$. A conditioned path is obtained implicitly by the integral

$$\check{r}_{\tilde{v}}(t) = \tilde{v}\int_{t_0}^{t} \frac{2}{\check{r}^2_{\tilde{v}}(\tau)} \int_0^{\check{r}_{\tilde{v}}(\tau)} \rho R_E(\rho,\tau)\mathrm{d}\rho\mathrm{d}\tau, \tag{4.5}$$

where the direction of $\check{\boldsymbol{r}}_{\tilde{v}}(t)$ is given by the direction of the conditioned velocity $\boldsymbol{v}(\boldsymbol{r}_0, t_0)_c$. We used the relation $g = \partial_r(rf)$ to introduce the reduced Eulerian velocity correlation $R_E(r,t) = f(r,t) + g(r,t) = 2f(r,t) + r\partial_r f(r,t)$ to give $f(r,t) = (1/r^2)\int_0^r \rho R_E(\rho,t)\mathrm{d}\rho$. The path in (4.5) is labelled by $\tilde{v}$ to emphasize the imposed condition. For small t we have $\check{r}_{\tilde{v}}(t) \approx \tilde{v}t$. We note that the integral $\int_0^{\check{r}_{\tilde{v}}(\tau)} \rho R_E(\rho,\tau)\mathrm{d}\rho\mathrm{d}\tau \to 0$, as $\check{r}_{\tilde{v}}(t) \to \infty$, as readily obtained using the expressions for f and g given before in terms of the correlation function of the stream function. Consequently f decreases faster than $1/r^2$.

The time variation of $\check{r}_{\tilde{v}}$ is shown in figure 3 for various values of $\tilde{v}$. We now assume as an approximation that an individual vortex in a given realization follows $\check{\boldsymbol{r}}_{\tilde{v}}(t)$. In order to obtain the characteristic function we then average $\exp[\mathrm{i}\boldsymbol{k}\cdot\check{\boldsymbol{r}}_{\tilde{v}}(t)]$ over all realizations of $\tilde{v}$ and let the reference positions be uniformly distributed. Here we can assume that for cases of interest the velocity probability density is a Gaussian with zero mean and known standard deviation, i.e. $P(\tilde{v}) = 2(\tilde{v}/\sigma^2)\exp(-(\tilde{v}/\sigma)^2)$. More generally the probability density can be obtained from results corresponding to (3.1). The *direction* of the imposed conditioned velocity is uniformly distributed in the interval $\{0, 2\pi\}$. With the present approximation the result is a closed expression

for R_E:

$$R_E(r,t) = \frac{1}{\sigma^2}\int_0^\infty kE(k)J_0(kr)\int_0^\infty 2(\tilde{v}/\sigma^2)\exp(-(\tilde{v}/\sigma)^2)J_0(k\check{r}_{\tilde{v}}(t))\mathrm{d}\tilde{v}\mathrm{d}k, \tag{4.6}$$

where $\check{r}_{\tilde{v}}(t)$ is given by (4.5). Equations (4.5)–(4.6) are solved numerically by an iterative procedure, in general. The initial condition at $t = t_0$ is given explicitly by the spectrum $E(\boldsymbol{k})$ through the use of (3.7) where for realistic conditions we assumed the divergence of the integral of (3.5) to be removed. A numerical solution of (4.5)–(4.6) is shown in figure 2(*b*). The result no longer necessarily follows the σt scaling of the simple approximation (3.10).

The error in assigning a conditionally averaged flow pattern to the actual flow velocity in a given realization can be estimated as

$$\begin{aligned} e^2 &= \langle(\check{\boldsymbol{v}}(\boldsymbol{r}_0+\boldsymbol{r},t_0+\tau)-\boldsymbol{v}(\boldsymbol{r}_0+\boldsymbol{r},t_0+\tau))^2\rangle \\ &= \langle v^2\rangle(1-R_E^2(r,\tau)). \end{aligned} \tag{4.7}$$

For small times and small spatial separations we have $e^2 \approx 2\langle v^2\rangle(1-R_E(r,\tau))$, see also (3.12). The error e is negligible in this limit. The maximum error $e^2 \approx \langle v^2\rangle$ is reached for large r or t where $R_E(r,t)$ vanishes. This maximum error is still only half of the one obtained by the approximation estimated by (3.12).

We find that $\check{\boldsymbol{v}}(\boldsymbol{r},\tau)$ as obtained from (4.4) goes to zero for $r \to \infty$. Therefore $\check{r}_{\tilde{v}}(t)$ increases only slowly as $t \to \infty$ with the present approximation (4.5). This observation can be made from (4.5), but was also directly seen in our numerical solutions of the equations, see also figure 3. For large times, the mean-square value $\langle\check{r}_{\tilde{v}}^2\rangle$ is increasing more slowly than the analytical result $\sim t$ obtained in (2.3). This limitation is expected to be of little consequence, however, since the oscillating contribution from the Bessel function in (4.6) makes the integral small even for finite values of $\check{r}_{\tilde{v}}$.

The improvement of the analysis by introducing the conditionally averaged flow can be substantiated by considering the mean-square error in using $\check{\boldsymbol{r}}_{\tilde{v}}$ as an estimate for the actual displacement $\boldsymbol{r}$. Thus, with angle brackets denoting averages over $\tilde{v}$ we find that $e_r^2 \equiv \langle(\check{\boldsymbol{r}}_{\tilde{v}}(t)-\boldsymbol{r}(t))^2\rangle$ for short times varies like $e_r^2 \sim t^4$ as in (3.13) since in this limit $\langle\check{\boldsymbol{r}}_{\tilde{v}}^2\rangle \approx \langle v^2\rangle t^2$ so the t^2-terms cancel as in (3.13). For large times on the other hand e_r^2 is dominated by $\langle r^2\rangle$ and we have $e_r^2 \sim t$ in this limit. We have no analytical expression for intermediate times as we had for (3.13). It is evident that the improved velocity estimate, $\check{\boldsymbol{v}}$, is just as good as the one used in (3.13) for short times, and in the long time limit it implies a considerably better estimate of the particle position compared to (3.13), so the approach seems worthwhile pursuing.

The method outlined here can be generalized by imposing additional conditions on one or more derivatives of the flow velocity at a reference point. The procedure for obtaining the corresponding conditional averages is in principle straight forward (Pécseli & Trulsen 1991*a*). It will be demonstrated in the following by a comparison with numerical simulations that the lowest-order approximation derived here actually gives quite satisfactory results.

The foregoing analysis is readily extended to the Lagrangian correlation functions. First we consider a frozen flow where formally all vortices are considered fixed at their (random) positions while continuing to 'spin'. The Eulerian correlation function $R_E(r)$ is now a function of spatial separations only. A test particle released in this flow will undergo random displacements and a Lagrangian correlation function can be defined for the velocity field sampled along its orbit. According to the previous

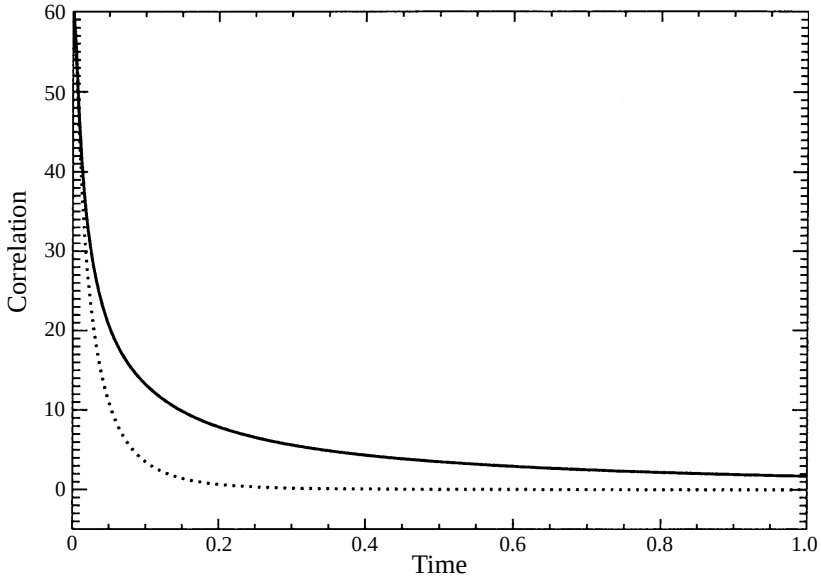

FIGURE 4. Analytically obtained Lagrangian correlation functions, where the dotted line gives the expression (3.11) based on the analysis of Wandel & Kofoed-Hansen while the solid line is obtained by numerical solution of (4.9) together with (4.5). The analytical expression for the Lagrangian integral time scale is complicated, but for the case shown by solid line we find numerically $\tau_L \approx 0.120$.

arguments the result is obtained following (4.6) as

$$R_L(t) = \frac{1}{\sigma^2}\int_0^\infty kE(k)\int_0^\infty 2(\tilde{v}/\sigma^2)\exp(-(\tilde{v}/\sigma)^2)J_0(k\check{r}_{\tilde{v}}(t))\mathrm{d}\tilde{v}\mathrm{d}k, \tag{4.8}$$

where $\check{r}_{\tilde{v}}(t)$ is determined by (4.5) with the time-independent $R_E(r)$ for the frozen flow inserted.

Although often applied as a simple model, such a frozen flow cannot serve as an illustration for physical flows since the individual vortices undergo random displacements which are not basically different from that of a test particle. The result (4.8) can be generalized by analogy to (3.11) to take into account the motion of vortices by assuming the probability density for relative velocities between test particles and vortices to be a Gaussian with standard deviation $\sigma\sqrt{2}$. The result is

$$R_L(t) = \frac{1}{\sigma^2}\int_0^\infty kE(k)\int_0^\infty (\tilde{v}/\sigma^2)\exp(-\tfrac{1}{2}(\tilde{v}/\sigma)^2)J_0(k\check{r}_{\tilde{v}}(t))\mathrm{d}\tilde{v}\mathrm{d}k, \tag{4.9}$$

again with $\check{r}_{\tilde{v}}(t)$ determined as a solution of (4.5) and where $R_E(r,t)$ is *a priori* given by the foregoing analysis. The result (4.9) is closely related to the Eulerian velocity correlation at zero spatial separation, just as (3.10) is related to (3.11). In figure 4 we show the result (4.9) as well as (3.11); they coincide for short time delays.

5. Numerical results

The model discussed in §1.1 was implemented numerically with periodic boundary conditions. The displacements of a large number of mutually convecting vortices are followed in time according to (1.9). The simulations are performed with a gridless $O(N^2)$ code. This makes the simulations rather time consuming, but avoids numerical

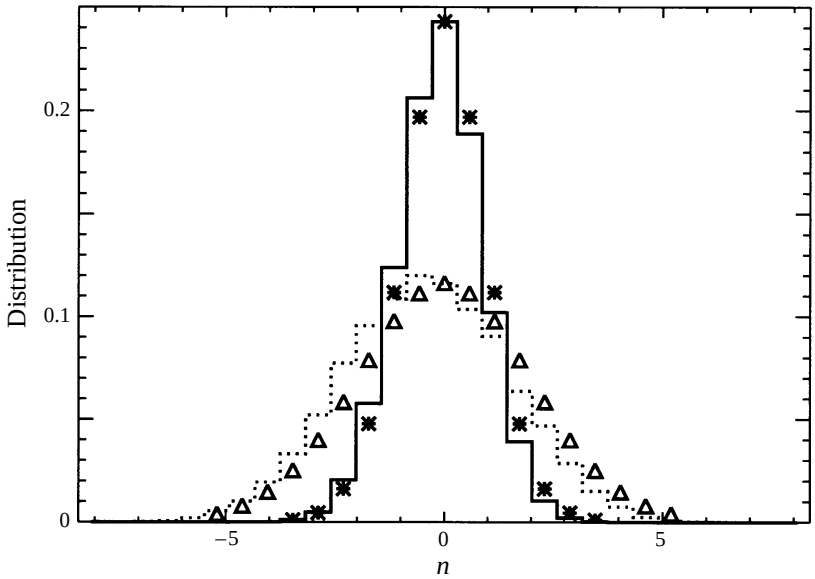

FIGURE 5. The solid line shows the distribution of the sum of the net number, n, of vortices defined as $\sum_i A_i/|A_i|$ within a square with area $\ell^2 = 1/4$ for $\mu = 12$. Asterixes give the value of $\exp(-\mu\ell^2)I_n(-\mu\ell^2)$ as a function of n. The asymmetry of the distribution is a measure of the statistical uncertainty of the result. The dotted line, with triangles for the analytical result, shows the same distribution, in the same simulation, for a square with area $\ell^2 = 1$.

diffusion which could invalidate the theoretical basis of the interpretation. The code uses a predictor–corrector method for the temporal evolution based on a variable timestep, which is determined by the smallest distance between any two vortices. The accuracy of the calculations is followed by evaluating the Hamiltonian (1.12) at regular time intervals. For convenience, the singularity of the K_0-function is smoothed out by a parabolic continuation within a small circle retaining a smooth first derivative at the circle. This smoothing is not logically necessary, but without it we may encounter large local flow velocities which necessitate unacceptably small timesteps for retaining the accuracy of the calculations. In the wavenumber spectrum the smoothing removes the energy in the largest wavenumbers, thus in effect corresponding to a truncation of the spectrum. As emphasized in §1.1, the Hamiltonian property of the model is retained for arbitrary functional variations of F in (1.12). This property is therefore not affected by the smoothing of the $K_0(r)$-function which enters the ideal model through (1.7).

In the initialization of the simulations we introduced vortices at positions determined by a standard random number generator. Placing vortices randomly but grouped with equal polarities within a checkerboard pattern, large positive values for the Hamiltonian can be obtained. Large negative values can be obtained by placing vortices of opposite polarity pairwise with large separation between pairs, see also Appendix B. The conservation of H given by (1.12) implies that such an ordering of vortices is likely to be retained for large values of $|H|$. For the present study we choose values of H close to zero, simply by repeating the initialization with new seeds for the random number generator until a value of H within a prescribed range was obtained.

The basic diagnostics used for analysing the results are probability densities for the two components of the flow velocity and the longitudinal and lateral velocity

N	$1/\lambda_R$	A	μ	σ_s	σ_s/σ_a	S	K
Rounding-off at radius 0.1							
400	1.5	1.0	4	4.55	0.96	−0.0451	3.74
800	1.5	$\sqrt{2}/2$	8	4.61	0.97	0.0018	3.44
1200	1.5	$\sqrt{3}/3$	12	4.71	0.99	0.0159	3.20
1200	1.5	$\sqrt{3}/3$	12	4.60	0.97	0.0110	3.12
1600	1.5	1/2	16	4.67	0.98	0.0343	3.02
Rounding-off at radius 0.05							
200	1.5	$\sqrt{2}$	8	5.71	1.03	0.0309	6.88
400	1.5	1.0	4	5.25	0.94	0.0229	4.65
800	1.5	$\sqrt{2}/2$	8	5.67	1.03	−0.0211	3.78
800	1.5	$\sqrt{2}/2$	8	5.57	0.99	−0.0326	4.12
1200	1.5	$\sqrt{3}/3$	12	5.52	0.99	-2.9×10^{-4}	3.66
1200	1.5	$\sqrt{3}/3$	12	5.40	0.96	1.5×10^{-2}	3.67

TABLE 1. Table of parameters for different simulations, where N is the number of vortices in the central simulation cell, and σ_s, σ_a are the standard deviations for one velocity component from simulations and analysis, respectively. Recall that here $\langle v^2\rangle = 2\sigma_s^2$. Cases listed with the same set of parameters, N, A and λ_R refer to different initializations of the random number generators.

correlations as functions of spatial and temporal separations. In addition figure 5 shows the distribution of the sum of the net number of vortices $\sum_j A_j/|A_j|$ within squares with area ℓ^2 and $\mu\ell^2 = 4$. For one vortex polarity only and with the assumption of the vortices being statistically independent, the analytical result is the binomial distribution

$$P_n = s^n(1-s)^{N-n}\begin{pmatrix} N \\ n \end{pmatrix},$$

where N is the total number of vortices in the simulation cell with area L^2, and $s = (\ell/L)^2$ is the probability of actually finding a vortex in the assigned subarea ℓ^2. In the limit where both N and L are large, the probability P_n is well approximated by a Poisson distribution $P_n = \exp(-\mu\ell^2)(\mu\ell^2)^n/n!$. For the case where the vortices take both polarities with equal probability and the vortices are of equal absolute strengths, $|A_j| = A$, we find after some calculations the corresponding result to be $P_n = \exp(-\mu\ell^2)I_n(\mu\ell^2)$ obtained again by assuming independent vortex positions. Asterixes in figure 5 represent the theoretical result. We note a quite satisfactory agreement. This result can be considered as an indirect test of the assumption of independent vortex positions.

In table 1 we show results obtained from the probability density for one velocity component (ideally, they are the same for x- and y-components). We use the skewness and kurtosis as indicators for the deviation from the ideal Gaussian distribution assumed in the analysis. For the present case the skewness is practically vanishing while a kurtosis of 3.62 is a sign of slightly enhanced probabilities for large velocity components compared with a Gaussian distribution. Table 1 shows the root-mean-square, σ, of one component of the velocity fluctuations for different μ. The corresponding kurtosis, K, and skewness, S, are given as well. The vortex strength A is varied together with vortex density μ so that μA^2 remains constant. Consequently we expect σ to remain constant for all μ, and K to approach the value 3 for large μ. For

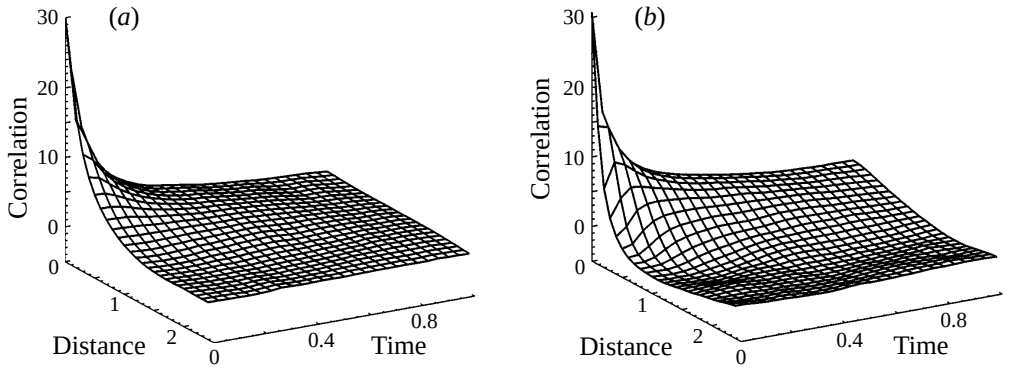

FIGURE 6. Eulerian correlation functions for velocity components obtained from the numerical simulations. In (*a*) we show the longitudinal correlations, in (*b*) the lateral correlations.

small values of μ, the kurtosis begins to increase noticeably, indicating significantly non-Gaussian fluctuations in velocity. We have $S = 0$ within the statistical uncertainty for all densities.

In figures 6(*a*) and 6(*b*) we show longitudinal and lateral Eulerian velocity correlations obtained from the simulations. Note that the lateral correlation function in figure 6(*b*), taken at zero time delay, integrates to zero as expected. The correlation between two orthogonal velocity components was also obtained for varying spatial and temporal separations. Ideally this correlation should be vanishing. Its actual value for the present simulation was in the range ± 0.4, much smaller than the r.m.s.-velocity. This number is an indicator of the effect of finite record lengths in our calculations. For comparison with the analytical results we show, in figure 7(*a*), the unnormalized reduced Eulerian velocity correlation function R_E. To facilitate the comparison with the analytical results we show in figure 7(*b*) the Eulerian correlation as a function of spatial separation for vanishing time delay with the analytical result given by the dashed line. Similarly, figure 7(*c*) gives the Eulerian correlation function as a function of time delay for vanishing spatial separation, again with the dashed line giving the analytical result. Three simulation results are included to give an indication of the statistical scatter. Two curves correspond to vortex densities of $\mu = 12$, one is for $\mu = 8$, see also table 1. The agreement between the analytical and numerical results is quite convincing. For lower vortex densities the agreement becomes noticeably worse as expected since the assumed Gaussian velocity distribution no longer applies, see also table 1.

Finally, figure 8 gives the unnormalized Lagrangian correlation function obtained by following a large number of test particles in the flow for the entire duration of the simulation. Also in this case three numerical curves are presented. The dashed line gives for comparison our analytical result as obtained in §4. The agreement between theoretical and numerical curves is not quite as good as in figure 7. For small time delays the agreement is, however, better than it might appear since, for the presentation, the Lagrangian correlation function was sampled with certain time intervals (this does not affect the accuracy of the calculations). On the figure we increased the time resolution for two of the cases shown. Concerning the Lagrangian integral time scale, we find numerically $\tau_L = 0.082 \pm 0.006$ for the present parameters.

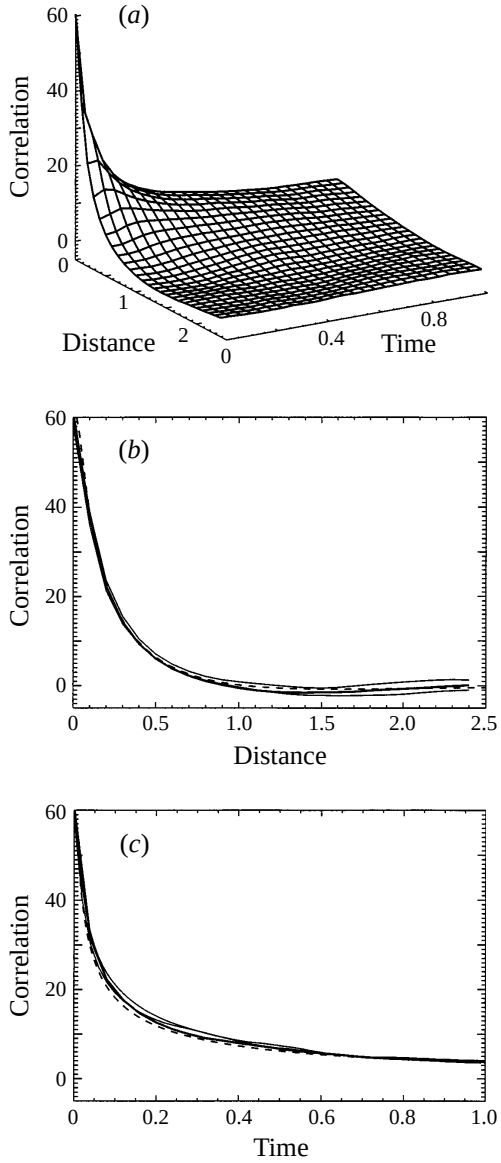

FIGURE 7. The reduced unnormalized Eulerian correlation function is shown in (*a*) to be compared with the analytical results in figure 2. In (*b*) the Eulerian correlation is shown as a function of spatial separation for vanishing time delay. Similarly, (*c*) gives the Eulerian correlation function as a function of time delay for vanishing spatial separation. The dashed lines give the analytical results. In (*b*) and (*c*) three curves are shown for different simulations, with the heavy line corresponding to (*a*).

5.1. *Comparison between analytical and numerical results*

From the value of the velocity correlations in figures 6(*a*) and 6(*b*) taken at zero delays we note that the standard deviations of the two velocity components are the same within a modest statistical uncertainty. The flow thus seems to have the assumed isotropy. The standard deviation deduced from the Lagrangian correlation function in figure 8 agrees with the corresponding results obtained from figure 7 in

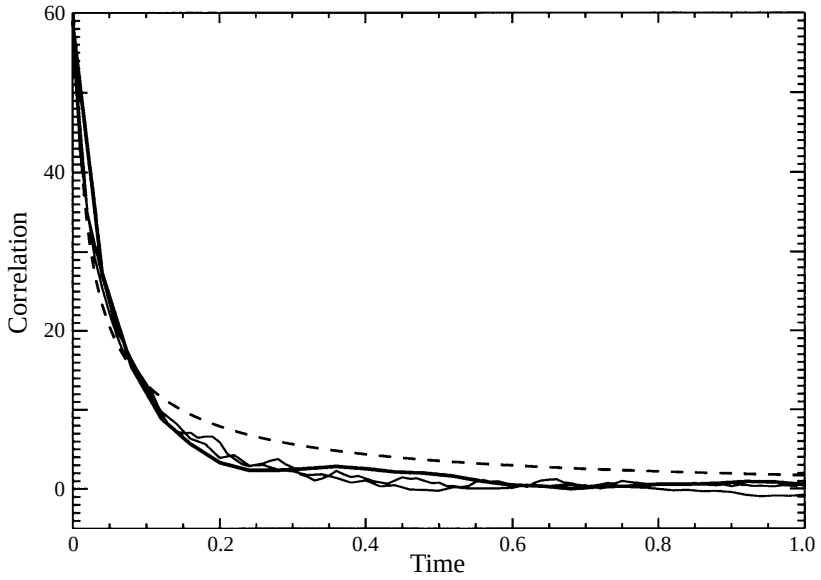

FIGURE 8. Unnormalized Lagrangian correlation function for the velocity sampled along test particle trajectories. See figure 4 for comparison. Dashed line gives the analytical result (4.9) from §4. Three curves are shown for different simulations, with the heavy line corresponding to figure 7(*a*).

agreement with the properties of incompressible flows. By comparing with figures 2 and 4 we find good agreement with the simple analytical results for this quantity, see also table 1. More important, however, is the very satisfactory agreement between the entire spatial and temporal variations of the analytical and numerical Eulerian correlation functions from figures 2(*b*) and 7(*a*), respectively, with details highlighted in figures 7(*b*) and 7(*c*). In particular the analytically obtained Eulerian length scale $\ell_E \approx 0.81$ is reproduced within the statistical uncertainty. It is evident that the result in figure 2(*a*) is adequate in predicting the short time variation of R_E, but fails otherwise. Concerning the Lagrangian correlations, we cannot claim the same excellent agreement, the Lagrangian correlation time being somewhat overestimated by our analytical results. Still, we find a satisfactory agreement with the simulations by using the result (4.9) as compared to (3.11) based on the analysis of Wandel & Kofoed-Hansen. Other methods, as discussed by for instance Gotoh *et al.* (1993), have been able to give better agreement between analytical results and numerical simulations for the Lagrangian correlations, but at the expense of a significant complication of the analysis.

Finally, the time variation of $\langle r^2 \rangle$ is shown in figure 9 with solid lines for three simulations. Interpreting figure 9 we recall the analytical result for the Lagrangian integral time scale $\tau_L \approx 0.120$ which overestimates the numerically obtained 0.082, see (2.3). For comparison, the dashed line shows the variation obtained from (2.2) with the analytical form of $R_L(t)$ inserted. The agreement is quite good, but it should be emphasized that this result concerns reduced information obtained by integrating the Lagrangian correlation function. Evidently, it is a more stringent test of the analysis directly to compare the theoretically obtained correlation functions with the numerical results.

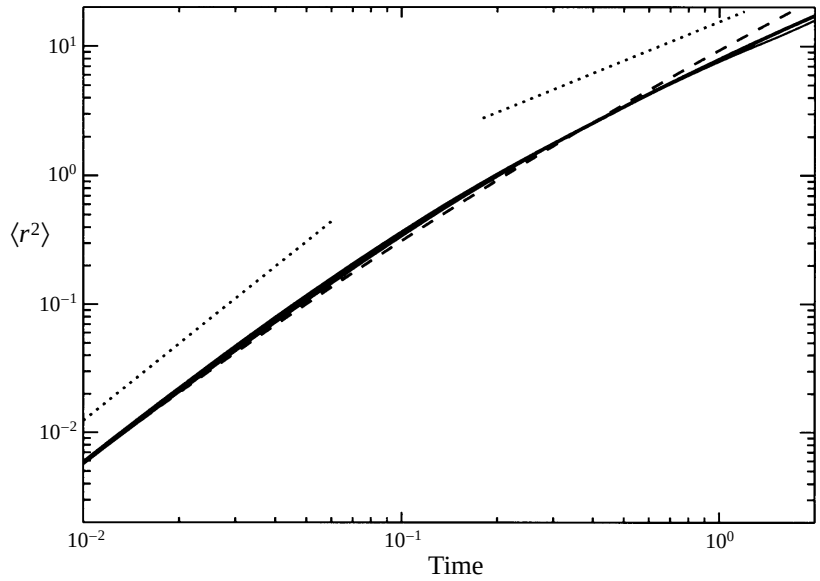

FIGURE 9. The numerically obtained time variation of $\langle r^2 \rangle$ is given by the solid line on a double logarithmic scale, the analytical result by a dashed line. Three numerical curves are shown for different simulations, with the heavy line corresponding to figure 7(*a*). The dotted lines give the slopes t^2 and t respectively. In interpreting the figure recall the analytical values $\ell_E = 0.81$ and $\tau_L = 0.120$.

6. Conclusions

In the present study we considered an autonomous vortex system which, in two spatial dimensions, models random flows with turbulence-like features. A multi-vortex simulation like the present one is a preferable alternative to a model consisting of randomly phased propagating waves which in general have no relation to the basic equations of the problem. Analytical results were obtained with the basic assumption that vortices are randomly distributed at all times. This assumption cannot be exact since the Hamiltonian property of the system imposes a correlation between all the vortices. For large negative values of H there is large probability of finding in the vicinity of any vortex another one with opposite polarity, see also the discussion in Appendix B. For large positive values of H, on the other hand, vortices with same polarity will be likely to cluster. For intermediate values, $H \approx 0$, we expect that the coupling between vortices is weak and therefore that the results of the first sections apply. It can be argued that this part of our analysis assumes the average lifetime of vortex pairs to be short. The good agreement between the analytical and numerical results concerning r.m.s.-velocity fluctuation levels and spatial correlations can be taken as an indication that the constraint imposed by constant H is not significant for the spatial distributions of vortices as long as $|H|$ is small. The results in figure 5 also support the assumption, since also in this case the analytical result is based on a random and independent distribution of vortices.

Our analytical results allowed a prediction of the full space–time variation of the Eulerian velocity correlation function without any free or adjustable parameters. We found that the agreement with the numerical results was fully satisfactory in the limit where the flow velocity at a given position is composed of contributions from many overlapping vortices, leading to the Gaussian velocity distribution assumed in the

analysis. For low densities, where the velocity probability density was significantly non-Gaussian, as measured by the kurtosis of the distribution, the agreement between analytical and numerical results became progressively worse, as expected. The agreement can, however, in that limit be substantially improved by making use of the general form (3.1). That analysis is, however, outside the scope of the present paper.

The analysis was extended to the Lagrangian correlation function, and acceptable agreement between analytical and numerical results was obtained. It is noteworthy that our analysis and simulations confirm that the Eulerian time scale is larger than its Lagrangian counterpart, in agreement with the expectations of Weinstock (1976), for instance. In particular the corresponding micro time-scales are related as $\tau_E \approx \sqrt{2}\tau_L$ to a first approximation. An alternative procedure for estimating the Lagrangian micro time-scale described by Monin & Yaglom (1975) is based on calculating the correlations of $\partial_t \boldsymbol{v} + \boldsymbol{v} \cdot \nabla \boldsymbol{v}$ in the Navier–Stokes equation, in terms of the correlations of pressure and of viscosity. This procedure has to be reformulated for the present problem where viscosity has been ignored.

The derivation of the Lagrangian correlation function for a frozen flow, like the one discussed by e.g. Kraichnan (1970), is a straightforward generalization of the derivation of the Eulerian correlation function. The generalization to the case with moving basic vortices was obtained by modelling the probability distribution of the relative velocities between vortices and test particles. This assumption cannot be tested directly, but it seems to give good results for the Lagrangian micro time scale. The disagreement for large time delays between our analytical result and those from the simulation can originate either from a shortcoming in the expression for the conditional particle displacement for large times, or alternatively from ignoring the correlation in the probability density of the relative velocity between test particles and vortices in the flow as outlined in §3.4, since these are the two central assumptions made. As the analytical expression for the Eulerian correlation function also agrees well with the numerical results for large time separations, the first one of these approximations is unlikely to be of importance; it equally enters the derivation of both Eulerian and Lagrangian correlations. The long tail in the analytical estimate for the Lagrangian correlation which disagrees with the numerical result is therefore most likely to be caused by the ignored velocity correlations, since this assumption entered only the Lagrangian analysis.

The actual form of the analytical expression for the Lagrangian correlation function allows an interpretation in terms of a wavenumber spectrum $E(k)$ multiplied by a time-varying filter. For instance, in the simple model (3.11) the filter is $\mathrm{e}^{-(\sigma k t)^2/2}$. Consequently, $\langle r^2 \rangle = t^2 \mathscr{V}^2(t)$ with $\mathscr{V}^2(t) = 2\int_0^\infty E(k) k \mathscr{C}(\sigma k t) \mathrm{d}k$ where

$$\mathscr{C}(\sigma k t) = \frac{1}{t}\int_0^t (1 - \tau/t)\mathrm{e}^{-(\sigma k \tau)^2/2}\mathrm{d}\tau$$

$$= \frac{\mathrm{e}^{-(\sigma k t)^2/2}}{(\sigma k t)^2} - \frac{1}{(\sigma k t)^2} + \frac{\sqrt{2\pi}}{2\sigma k t}\mathrm{erf}\left(\tfrac{1}{2}\sqrt{2}\sigma k t\right).$$

Also, the more general result (4.9) can formally be interpreted in terms of large wavenumbers being filtered away for increasing times. For small times all Fourier components contribute to $R_L(\tau)$ and therefore to the mean-square particle displacement $\langle r^2 \rangle$ in (2.2). At later times the contributions from the largest wavenumbers are quenched by the filter, and ultimately only the smallest k contribute to the ran-

dom displacement of the test particle with respect to its origin of release (Pécseli & Mikkelsen 1985). From the definition of $\mathscr{V}$, the requirement that $E(k) \to 0$ for $k \to 0$ is evident. The unshielded vortex model fails to satisfy this requirement, as discussed in different contexts by Taylor & McNamara (1971). A random flow generated by a superposition of unshielded vortices has a long tail on the Lagrangian correlation function which gives rise to a diffusion which is faster than $t^{1/2}$.

The idea of turbulent diffusion being caused by successively larger and larger scales seems intuitively appealing, but it must be emphasized that the Fourier components are not to be interpreted as individually propagating weakly coupled waves. In the present model and in the simulations only a large number of identical vortices are present, and a particle is displaced as a result of the entire simultaneous contribution from all the vortices.

The analysis can be systematically extended, although the practical problems in doing so are not to be underestimated. Higher-order terms can be included in the estimator for the conditional vortex trajectory, and the imposed conditions can be extended. These corrections will depend on correlations of higher order, i.e. triple correlations. Here, by retaining only the first terms, we attempted to optimize the use of the information in the wavenumber power spectrum for estimating the full space–time variation of the Eulerian velocity correlation function as well as the time variation of its Lagrangian counterpart. The good overall agreement between the numerical and analytical results also gives support to the basic idea of a closure based on conditional statistics.

The present study was based on a Hamiltonian model which allowed a prediction of wavenumber spectra as well as Eulerian and Lagrangian velocity correlations for this two-dimensional random flow. The analysis is parameter-free in the sense that once the basic vortex characteristics and a vortex density are chosen to set up the simulation, then there are no free parameters left for adjusting the agreement between analytical and numerical results. The present results can also be interpreted as a prediction of these correlations, provided the wavenumber spectrum is *a priori* given, for instance, from measurements. This property of the results remains to be studied in detail. Numerical simulations combined with the appropriate analysis are in progress.

We thank Professor M. Kono for valuable discussions. This work was supported in part by the Norwegian Research Council for Science and the Humanities.

Appendix A. Conditional averaging

In this Appendix we summarize some aspects of the closure based on conditional averaging discussed in the main text. First it may be worthwhile briefly to discuss some basic properties of the vortex distribution function $D_N(\boldsymbol{r}_1, \boldsymbol{r}_2, \ldots, \boldsymbol{r}_N, t)$ in a $2N$-dimensional phase-space, where $\boldsymbol{r}_j$ is the Eulerian coordinate of the jth vortex at time t. Liouville's equation takes the form

$$\frac{\partial D_N}{\partial t} + \sum_{i=1}^{N} \sum_{j=1}^{N}{}' \nabla_i \cdot (\boldsymbol{v}_{i,j} D_N) = 0, \tag{A 1}$$

where the prime indicates that $j \neq i$ in the double summation. The normalization is $\int \cdots \int_{-\infty}^{\infty} D_N \mathrm{d}\boldsymbol{r}_1 \cdots \mathrm{d}\boldsymbol{r}_N = 1$, with $D_N \geqslant 0$. We have introduced $\boldsymbol{v}_{i,j} \equiv \boldsymbol{v}_i(|\boldsymbol{r}_j - \boldsymbol{r}_i|)$ from (1.11) with $\boldsymbol{v}_i(|\boldsymbol{r}|) = A_i \nabla F(|\boldsymbol{r}|) \times \hat{\boldsymbol{b}}$. In general we cannot assume symmetry of the

distribution function with respect to permutations of individual vortex positions

$$D_N(\boldsymbol{r}_1,\ldots,\boldsymbol{r}_i,\ldots,\boldsymbol{r}_j,\ldots,\boldsymbol{r}_N,t) = D_N(\boldsymbol{r}_1,\ldots,\boldsymbol{r}_j,\ldots,\boldsymbol{r}_i,\ldots,\boldsymbol{r}_N,t), \tag{A 2}$$

since the vortices, labelled j and i can have different strengths $A_j \neq A_i$. For the general case we have assumed that the A have a continuous distribution, including both signs. Without the assumption (A 2), however, little can be done to reduce (A 1). Here it is therefore assumed that all $A_j = A$, and that (A 2) is indeed fulfilled. Introducing the standard notation

$$f_s(\boldsymbol{r}_1,\boldsymbol{r}_2,\ldots,\boldsymbol{r}_s,t) = \mathscr{A}^s \int\cdots\int_{-\infty}^{\infty} D_N(\boldsymbol{r}_1,\boldsymbol{r}_2,\ldots,\boldsymbol{r}_N,t)\mathrm{d}\boldsymbol{r}_{s+1}\cdots\mathrm{d}\boldsymbol{r}_N$$

with $\mathscr{A}$ being the area of the system, (A 1) is integrated to give the well-known expression

$$\frac{\partial f_s}{\partial t} + \sum_{i=1}^{s}{\sum_{j=1}^{s}}' \nabla_i\cdot(\boldsymbol{v}_{i,j}f_s) + \frac{(N-s)}{\mathscr{A}}\sum_{i=1}^{s}\nabla_i\cdot\int_{-\infty}^{\infty}\boldsymbol{v}_{i,s+1}f_{s+1}\mathrm{d}\boldsymbol{r}_{s+1} = 0. \tag{A 3}$$

For large N and small s the approximation $(N-s)/\mathscr{A} \approx \mu$ is used. By normalizing distance with the Rossby radius λ_R a small expansion parameter $1/(\mu\lambda_R^2)$ can be identified. Ignoring vortex correlations by approximating

$$f_2(\boldsymbol{r}_1,\boldsymbol{r}_2,t) \approx f_1(\boldsymbol{r}_1,t)f_1(\boldsymbol{r}_2,t), \tag{A 4}$$

the equation for f_1 is obtained in the form

$$\frac{\partial f_1}{\partial t} + \boldsymbol{v}\cdot\nabla f_1 = 0, \tag{A 5}$$

with $\boldsymbol{v}(\boldsymbol{r}_1,t) = \mu\int_{-\infty}^{\infty}\boldsymbol{v}_{1,2}f_1(\boldsymbol{r}_2,t)\mathrm{d}\boldsymbol{r}_2$. Explicit use has been made of the incompressibility of the flow. The result (A 5) is the continuity equation for the plane perpendicular to $\boldsymbol{\Omega}$. For cases where the A can assume a finite number of values a condition similar to (A 2) can be imposed on each vortex type. With correlations ignored, ultimately (A 5) is obtained as a general result. Details of these arguments are given by for instance Novikov (1975) or Montgomery (1975). The independence assumption (A 4) means that the evolution of the probability density for the vortex with label 1 is independent of the actual presence of another one at position $\boldsymbol{r}_2$. Explicit use of this assumption was made in the main text.

The nonlinear equation (A 5) can be solved in special cases only. A considerable simplification is obtained by assuming that the statistical properties of the flow $\boldsymbol{v}$ are given *a priori*. The dispersion of one vortex in this flow can be analysed. This vortex can then be interpreted as a passive test particle. The argument can be substantiated by noting that in the limit of many overlapping vortices the contribution of one can be removed from the series (1.9) without noticeable consequences for the statistical properties of the flow as such. A simplified analysis of the dynamics of randomly distributed vortices was discussed by Kono & Horton (1991). For randomly varying velocity fields an approximate solution can be obtained by considering first a conditioned representation of $\boldsymbol{v}$. Assume that the velocity field is known with certainty at a reference position $\boldsymbol{r}_0$ at a reference time t_0. The entire flow field can then be estimated subject to this condition. This estimate is denoted $\check{\boldsymbol{v}}$. The actual (conditioned) flow field then becomes $\boldsymbol{v}(\boldsymbol{r},t)_c = \check{\boldsymbol{v}}(\boldsymbol{r},t) + \boldsymbol{\vartheta}(\boldsymbol{r},t)$ as before, where $\boldsymbol{\vartheta}(\boldsymbol{r},t)$ is a random correction, subject to the condition $\boldsymbol{\vartheta}(\boldsymbol{r}_0,t_0) = 0$.

We now look for a solution for the conditionally averaged Green function. The Green function, $\mathscr{G}_c$, for individual realizations is fluctuating over the conditionally selected subensemble with the basic equation being $\partial_t \mathscr{G}_c + (\check{\boldsymbol{v}}(\boldsymbol{r},t) + \boldsymbol{\vartheta}(\boldsymbol{r},t)) \cdot \nabla \mathscr{G}_c = 0$ for the conditionally selected subensemble with initial condition $\mathscr{G}_c(\boldsymbol{r}, t_0 \mid \boldsymbol{r}_0, t_0) = \delta(\boldsymbol{r} - \boldsymbol{r}_0)$. Introducing the decomposition into averaged and fluctuating parts G_c and g, we have the equations

$$\frac{\partial G_c}{\partial t} + \check{\boldsymbol{v}} \cdot \nabla G_c = -\langle \boldsymbol{\vartheta} \cdot \nabla g \rangle_c \tag{A 6}$$

with initial condition $G_c(\boldsymbol{r}, t_0 \mid \boldsymbol{r}_0, t_0) = \delta(\boldsymbol{r} - \boldsymbol{r}_0)$, and

$$\frac{\partial g}{\partial t} + \check{\boldsymbol{v}} \cdot \nabla g + \boldsymbol{\vartheta} \cdot \nabla G_c = -\boldsymbol{\vartheta} \cdot \nabla g + \langle \boldsymbol{\vartheta} \cdot \nabla g \rangle_c \tag{A 7}$$

with initial condition $g(\boldsymbol{r}, t_0 \mid \boldsymbol{r}_0, t_0) = 0$. The subscript c on the averaging serves as a reminder that the averaging is to be carried out over the conditionally selected subensemble. For the general case the lowest-order solution is obtained when the right-hand side of (A 7) is ignored, retaining only the coupling between fluctuations and averaged quantities in that equation (Orszag 1969). Then (A 7) can be solved to give the approximation

$$\begin{aligned} \frac{\partial G_c(\boldsymbol{r}, t \mid \boldsymbol{r}_0, t_0)}{\partial t} &+ \check{\boldsymbol{v}}(\boldsymbol{r}, t) \cdot \nabla G_c(\boldsymbol{r}, t \mid \boldsymbol{r}_0, t_0) \\ &= \int_{t_0}^{t} \mathrm{d}s \int_{-\infty}^{\infty} \mathrm{d}\boldsymbol{\xi}\, \nabla G_0(\boldsymbol{r}, t \mid \boldsymbol{\xi}, s) \cdot \langle \boldsymbol{\vartheta}(\boldsymbol{r}, t) \boldsymbol{\vartheta}(\boldsymbol{\xi}, s) \rangle_c \cdot \nabla_{\xi} G_c(\boldsymbol{\xi}, s \mid \boldsymbol{r}_0, t_0), \end{aligned} \tag{A 8}$$

with the lowest-order Green function G_0 satisfying the equation

$$\frac{\partial G_0(\boldsymbol{r}, t \mid \boldsymbol{r}_0, t_0)}{\partial t} + \check{\boldsymbol{v}}(\boldsymbol{r}, t) \cdot \nabla G_0(\boldsymbol{r}, t \mid \boldsymbol{r}_0, t_0) = 0. \tag{A 9}$$

With the appropriate initial condition, the equation for G_0 can be solved to give

$$G_0(\boldsymbol{r}, t \mid \boldsymbol{r}_0, t_0) = \delta \left(\boldsymbol{r} - \boldsymbol{r}_0 - \int_{t_0}^{t} \boldsymbol{u}(\boldsymbol{r}(\tau), \tau) \mathrm{d}\tau \right), \tag{A 10}$$

where $\boldsymbol{u}(\boldsymbol{r}(t), t) = \check{\boldsymbol{v}}(\boldsymbol{r}_0 - \int_{t_0}^{t} \check{\boldsymbol{v}}(\boldsymbol{r}(\tau), \tau) \mathrm{d}\tau, t)$ with $\mathrm{d}\boldsymbol{r}(t)/\mathrm{d}t = \check{\boldsymbol{v}}(\boldsymbol{r}, t)$. The right-hand side of (A 8) can be simplified somewhat by use of (A 10). Finally, the averaged unconditioned Green function is obtained from G_c by averaging over the imposed conditions, assuming that their probability density is known.

The analysis assumes expressions for the conditional averages $\check{\boldsymbol{v}}(\boldsymbol{r}, t)$ and $\langle \boldsymbol{\vartheta}(\boldsymbol{r}, t) \boldsymbol{\vartheta}(\boldsymbol{\xi}, s) \rangle_c$ to be explicitly known. As discussed in §4 the first of these can be expressed to a first approximation in terms of the two-point two-time correlation function. Similarly we obtain $\langle \boldsymbol{\vartheta}(\boldsymbol{r}, t) \boldsymbol{\vartheta}(\boldsymbol{\xi}, s) \rangle_c = \langle \boldsymbol{v}(\boldsymbol{r}, t)_c \boldsymbol{v}(\boldsymbol{\xi}, s)_c \rangle_c - \check{\boldsymbol{v}}(\boldsymbol{r}, t) \check{\boldsymbol{v}}(\boldsymbol{r}, t)$, by expressing

$$\begin{aligned} &\check{R}_{jk}(\boldsymbol{r}_0 + \boldsymbol{\rho}, t_0 + t, \boldsymbol{r}_0 + \boldsymbol{\xi}, t_0 + s) \\ &\quad \equiv \langle v_j(\boldsymbol{r}_0 + \boldsymbol{\rho}, t_0 + t)_c v_k(\boldsymbol{r}_0 + \boldsymbol{\xi}, t_0 + s)_c \rangle_c \\ &\quad = Q_{jk}(\boldsymbol{\rho}, t, \boldsymbol{\xi}, s) + S_{jk\ell}(\boldsymbol{\rho}, t, \boldsymbol{\xi}, s) \tilde{v}_{\ell}(\boldsymbol{r}_0, t_0) \\ &\qquad + T_{jk\ell m}(\boldsymbol{\rho}, t, \boldsymbol{\xi}, s) \tilde{v}_{\ell}(\boldsymbol{r}_0, t_0) \tilde{v}_m(\boldsymbol{r}_0, t_0) \ldots, \end{aligned}$$

where $\tilde{v}_k(\boldsymbol{r}_0, t_0)$ is the kth component of the conditioned velocity vector and $\boldsymbol{v}(\boldsymbol{r}, t)_c$ is again the velocity in one realization of the conditioned subensemble, $\boldsymbol{v}(\boldsymbol{r}_0, t_0)_c = \tilde{\boldsymbol{v}}$. The notation is chosen to emphasize that the conditionally selected subensemble is

in general neither stationary nor homogeneous. The elements of Q_{jk}, the coefficient tensor $S_{jk\ell}$, as well as higher-order coefficients are found by minimizing

$$e_{jk}^2 = \langle (\check{R}_{jk}(\boldsymbol{r}_0 + \boldsymbol{\rho}, t_0 + t, \boldsymbol{r}_0 + \boldsymbol{\xi}, t_0 + s) - v_j(\boldsymbol{r}_0 + \boldsymbol{\rho}, t_0 + t) v_k(\boldsymbol{r}_0 + \boldsymbol{\xi}, t_0 + t))^2 \rangle$$

as in §4, see also Adrian (1977). For the present problem the first term in the series will no longer suffice as an approximation. The procedure is discussed more generally by Pécseli & Trulsen (1991*a*) although that work did not distinguish fluctuations in the conditionally selected subensemble. Their results are, however, easily modified. Diffusion of conditionally released particles was also discussed by Philip (1968).

The simplest case is the random convection model, with $\boldsymbol{v} = \boldsymbol{v}_1$ =const. in each realization but randomly varying over the ensemble, corresponding to a simple Galileian translation of each individual realization. Then $\check{\boldsymbol{v}}(\boldsymbol{r}, t) = \boldsymbol{v}_1$ and $\vartheta = 0$. Consequently $G_c(\boldsymbol{r}, t \,|\, \boldsymbol{r}_0, t_0) = \delta(\boldsymbol{v}_1(t - t_0) + \boldsymbol{r} - \boldsymbol{r}_0)$. The statistical distribution of the velocities, $P(\boldsymbol{v}_1)$, is assumed to be known. It can be measured, predicted by a model as in §4, or known to be a Gaussian from first principles. The unconditioned averaged Green function is then obtained by averaging over all possible conditions, here as $G = \int G_c P(\boldsymbol{v}_1) \mathrm{d}\boldsymbol{v}_1 = P((\boldsymbol{r} - \boldsymbol{r}_0)/(t - t_0))/(t - t_0)$. This is however the exact result for this particular case, which can be solved directly from the basic equation. The results (A 8) and (A 9) with (A 10) thus give the exact result when applied to the random convection model mentioned before, just as the corresponding equations do when applied to the random acceleration problem discussed by Pécseli & Trulsen (1991*a*). It is plausible that the shortcomings of the Eulerian direct interaction approximation (EDIA) in treating random Galileian translations (Kraichnan 1964; Leslie 1973) can be remedied by using a conditionally selected subensemble.

A considerable generalization and improvement can be expected by replacing G_0 in (A 8) by the transition probability G_c itself. The arguments are quite similar to those put forward by Orszag (1969) in discussions of the random-coupling model, and they will not be given here. This expected improvement will however be obtained at the expense of a nonlinear equation for G_c.

The unconditioned Green function is obtained by averaging G_c over all realizations of the imposed conditions, which quite generally will be on $\boldsymbol{v}(\boldsymbol{r}_0, t_0)$, $\nabla \boldsymbol{v}(\boldsymbol{r}_0, t_0), \ldots$, requiring the relevant joint probability densities to be known. The conditional averages are in principle measurable quantities, but it is a great practical simplification that they can expressed in terms of correlation functions as shown by an example in §4. More general cases were discussed by Pécseli & Trulsen (1991*a*) in terms of series expansions as in §4. In particular, Pécseli & Trulsen (1991*b*) compared the analytically obtained estimates with actual results from a numerical simulation and found that even for significantly non-Gaussian cases a few terms in the series expansion would be sufficient. It is important that the correlations and probability densities entering the construction for these higher-order corrections are Eulerian, i.e. even in the absence of *a priori* analytical expressions they are amenable to straightforward measurements, at least within some uncertainty. Although the procedure outlined here is in principle feasible for any set of imposed conditions, it is evidently of great practical advantage that the simplest condition suffices, i.e. the convergence of the method seems to be rapid.

The approximation used in §4 consists of approximating G_c by G_0, since it was argued that, at least for small times and spatial separations, the error on the estimate was small. It is an interesting question how much the results would be improved by use of the first-order smoothing approximation and, ultimately, by the random-coupling

approximation. We shall not deal with theses problems here, but only mention that the analysis can be generalized to inhomogeneous and anisotropic conditions as well. The conditional averages are readily modified although then the relevant correlations will depend on both spatial coordinates. Also, non-stationary conditions can be considered with additional complications in the analysis.

Appendix B. Comments on double vortex systems

The analysis in the main part of the paper was explicitly restricted to the case where the Hamiltonian was close to zero. Only in this case can it be argued that the correlation between vortices can be ignored to a first approximation. Large negative values of the Hamiltonian can be analysed by somewhat similar arguments, but the results cannot be obtained in a simple closed form. It may be instructive to discuss this limiting case also to emphasize the differences from the one already considered. In the foregoing analysis, the basic building stone of the flow field was the individual vortex described by the K_0-function, apart from the rounding-off at the origin. By an analysis entirely similar to the one used before we may obtain the wavenumber spectrum for a system derived by a random superposition of double vortices consisting of two single vortices of opposite polarity a distance p apart. The initial orientation of the vortex pairs is assumed uniformly distributed over angles with respect to any coordinate-axis. Again it is simplest to derive the correlations of the stream function variation first. The associated variation of one basic vortex pair is $AF(\boldsymbol{r}+\frac{1}{2}\boldsymbol{p})-AF(\boldsymbol{r}-\frac{1}{2}\boldsymbol{p})$. The result is

$$R_\Phi(\xi)=2\left[\mathscr{R}(\xi)-\frac{1}{2\pi}\int_0^{2\pi}\mathscr{R}\left(\left(\xi^2+p^2+2p\cos\theta\right)^{1/2}\right)\mathrm{d}\theta\right], \tag{B 1}$$

where $\mathscr{R}(\xi)=\mu A^2\int_{-\infty}^{\infty}F(\boldsymbol{r})F(\boldsymbol{r}-\boldsymbol{\xi})\mathrm{d}\boldsymbol{r}$. The integration over θ comes from the averaging over all dipole orientations. From (B 1) the velocity correlation tensor is readily obtained.

The full space–time variation of the correlation function of the stream function is easily obtained since each double vortex has a constant velocity, predetermined by its distance p, i.e. $v_p=(|A|/2\pi\lambda_R)K_1(p/\lambda_R)$. This is the major difference from the problem considered previously, where the basic structure did not have a propagation of its own, only one due to the combined effect of the others. For the present case we obtain

$$R_E(r,t)=\frac{1}{\sigma^2}\int_0^{\infty}E(k)J_0(kr)J_0(kv_pt)k\mathrm{d}k\,, \tag{B 2}$$

with $E(k)$ obtained as the Fourier transform of (B 1). The velocity probability densities of the flow, $P(v_x)$ and $P(v_y)$, are readily derived from (3.1). In the present case the density μ evidently has to be small in order to retain long-lived double vortices. Consequently, $P(v_x)$ and $P(v_y)$ are not close to Gaussian distributions.

The result (B 1) is applicable only in somewhat extreme cases where the double vortices do not interact upon collisions to change p, or never collide at all. In reality, after some time and a large number of collisions, the internal distances will be statistically distributed. The evolution of the distribution of pair separations, p, will depend on the constraints imposed by the conserved quantities for the system, H in particular. Given this distribution, the analysis can then be made complete, at least for a dilute gas of double vortices, by averaging over all p. We cannot, however, predict this distribution from first principles. It is on the other hand

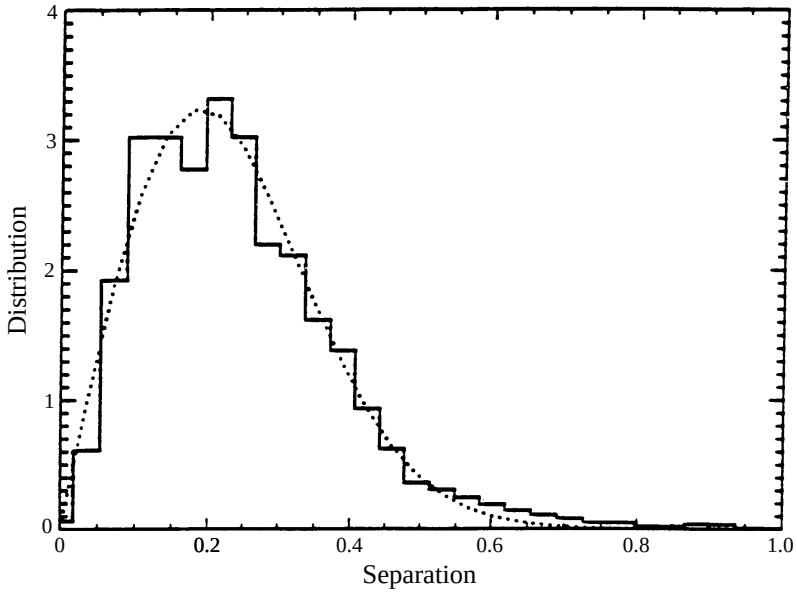

FIGURE 10. Distribution of the internal separation, p, of double vortices obtained after the relaxation of a system where p was initially distributed uniformly in the interval [0.1; 0.4], for a value of $H \ll 0$. Distributions at many timesteps are averaged. The histogram is normalized to unit area, and can be interpreted as a probability density for vortex separations, p, which we normalized by $L/(2N)^{1/2}$, where $2N$ is the number of vortices in the system. The vortex amplitudes are $\pm\sqrt{2}$ with $N = 100$ giving a density of $1/2$. The dotted line gives the best fit for a Rayleigh distribution.

measurable with a result shown in figure 10. Apparently the probability density $P(p)$ is well approximated by a Rayleigh distribution, given by a dotted line, although we see no *a priori* reason to expect this. The figure shown is representative of all our simulations concerning this particular problem. In all cases we find that the Rayleigh distribution gives a good overall fit, but the 'tail' is in most cases slightly over-represented.

REFERENCES

ADRIAN, R. J. 1977 On the role of conditional averages in turbulence theory. In *Turbulence in Liquids: Proc. 4th Biennial Symp. on Turbulence in Liquids* (ed. J. L. Zakin & G. K. Patterson), pp. 323–332. Science Press, Princeton, NJ.

ADRIAN, R. J. 1979 Conditional eddies in isotropic turbulence. *Phys. Fluids* **22**, 2065–2070.

BABIANO, A., BOFFETTA, G., PROVENZALE, A. & VULPIANI, A. 1994 Chaotic advection in point vortex models and two–dimensional turbulence. *Phys. Fluids* **6**, 2465–2474.

CHARNEY, J. G. 1948 On the scale of atmospheric motions. *Geophys. Publ. Norwegian Acad. Sci.* **17**, 3–17.

CORRSIN, S. 1960 Progress report on some turbulent diffusion research. *Adv. Geophys.* **6**, 161–164.

FUNG, J. C. H., HUNT, J. C. R., MALIK, N. A. & PERKINS, R. J. 1992 Kinematic simulation of homogeneous turbulence by unsteady random Fourier modes. *J. Fluid Mech.* **236**, 281–318.

GOTOH, T., ROGALLO, R. S., HERRING, J. R. & KRAICHNAN, R. H. 1993 Lagrangian velocity correlations in homogeneous isotropic turbulence. *Phys. Fluids* A **5**, 2846–2864.

HASEGAWA, A., IMAMURA, T., MIMA, K. & TANIUTI, T. 1978 Stationary spectrum of pseudo–three–dimensional electrostatic turbulence in magnetized plasmas. *J. Phys. Soc. Japan* **45**, 1005–1010.

HASEGAWA, A., MACLENNAN, C. G. & KODAMA, Y. 1979 Nonlinear behavior and turbulence spectra of drift waves and Rossby waves. *Phys. Fluids* **22**, 2122–2129.

Hay, J. S. & Pasquill, F. 1960 Diffusion from a continuous source in relation to the spectrum and scale of turbulence. *Adv. Geophys.* **6**, 345–365.

Horton, W. & Hasegawa, A. 1994 Quasi-two-dimensional dynamics of plasmas and fluids. *Chaos* **2**, 227–251.

Kofoed-Hansen, O. & Wandel, C. F. 1967 On the relation between Eulerian and Lagrangian averages in the statistical theory of turbulence. *Risø Rep.* 50.

Kono, M. & Horton, W. 1991 Point vortex description drift wave vortices: dynamics and transport. *Phys. Fluids* B **3**, 3255–3262.

Kraichnan, R. 1959 The structure of isotropic turbulence at very high Reynolds numbers. *J. Fluid Mech.* **5**, 497–543.

Kraichnan, R. 1964 Kolmogorov's hypothesis and Eulerian turbulence theory. *Phys. Fluids* **7**, 1723–1734.

Kraichnan, R. 1970 Diffusion by a random velocity field. *Phys. Fluids* **13**, 22–31.

Leonard, A. 1980 Vortex methods for flow simulation. *J. Comput. Phys.* **37**, 289–335.

Leslie, D. C. 1973 *Developments in the Theory of Turbulence*. Oxford University Press.

Lynov, J. P., Nielsen, A. H., Pécseli, H. L. & Rasmussen, J. J. 1991 Studies of the Eulerian–Lagrangian transformation in two-dimensional random flows. *J. Fluid Mech.* **224**, 485–505.

McComb, W. D. 1990 *The Physics of Fluid Turbulence*. Clarendon.

Monin, A. S. & Yaglom, A. M. 1975 *Statistical Fluid Dynamics,* Vol. 2. MIT Press.

Montgomery, D. 1975 Magnetized plasma models. In *Plasma Physics — Physique des Plasmas* (ed. C. DeWitt & J. Peyraud), pp. 431–535. Gordon and Breach.

Morikawa, G. K. 1960 Geostrophic vortex motion. *J. Metl.* **17**, 148–158.

Novikov, E. A. 1975 Dynamics and statistics of a system of vortices. *Zh. Eksper. Teor. Fiz.* **68**, 1868–1882 (Engl. transl. *Sov. Phys. JETP* **41**, 937–943).

Onsager, L. 1949 Statistical hydrodynamics. *Nuovo Cimento Suppl.* **6**, 279–287.

Orszag, S. A. 1969 Stochastic acceleration by strong electric fields. In *Proc. Symposium on Turbulence in Fluids and Plasmas*, pp. 17–28. Polytechnic, New York.

Panofsky, H. A. & Dutton, J. A. 1984 *Atmospheric Turbulence*. John Wiley.

Pécseli, H. L. & Mikkelsen, T. 1985 Turbulent diffusion in two–dimensional strongly magnetized plasmas. *J. Plasma Phys.* **34**, 77–94.

Pécseli, H. L. & Trulsen, J. 1991*a* Phase–space diffusion in turbulent plasmas: the random acceleration problem revisited. *Phys. Fluids* B **3** 3271–3276.

Pécseli, H. L. & Trulsen, J. 1991*b* Analytical expressions for conditional averages: a numerical test. *Physica Scr.* **43** 503–507.

Philip, J. R. 1968 Diffusion by continuous movements. *Phys. Fluids* **11**, 38–42.

Rice, S. O. 1944 Mathematical analysis of random noise. *Bell System Tech. J.* **23**, 282–332. (Reprinted in *Selected Papers on Noise and Stochastic Processes* (ed. N. Wax) Dover 1954.)

Rice, S. O. 1945 Mathematical analysis of random noise. *Bell System Tech. J.* **24**, 46–156. (Reprinted in *Selected Papers on Noise and Stochastic Processes* (ed. N. Wax) Dover 1954.)

Sarpkaya, T. 1989 Computational Methods With Vortices — the 1988 Freeman Scholar Lecture. *Trans. ASME. J. Fluids Engng* **111**, 5–52.

Smith, F. B. 1968 Conditioned particle motion in a homogeneous turbulent field. *Atmos. Environ.* **2**, 491–508.

Taylor, J. B. & McNamara, B. 1971 Plasma diffusion in two dimensions. *Phys. Fluids* **14**, 1492–1499.

Tennekes, H. & Lumley, J. L. 1972 *A First Course in Turbulence*. MIT Press.

Wandel, C. F. & Kofoed-Hansen, O. 1962 On the Eulerian–Lagrangian transform in the statistical theory of turbulence. *J. Geophys. Res.* **67**, 3089–3093.

Weinstock, J. 1976 Lagrangian–Eulerian relation and the independence approximation. *Phys. Fluids* **19**, 1702–1711.